Solution of the mean field equations for spontaneous fission

G. Puddu* and J. W. Negele

Center for Theoretical Physics, Laboratory for Nuclear Science and Department of Physics,
Massachusetts Institute of Technology, Cambridge, Massachusetts 02139
(Received 4 September 1986)

A new iterative method is used to solve the self-consistent periodic mean field equations governing nuclear fission. A general filter method is introduced to interactively refine an initial approximation, and its stability and convergence are analyzed. The basic ideas are illustrated for the familiar static Hartree equations and generalized to address the unique aspects of the mean field tunneling problem. The method is applied to an illustrative self-consistent fission problem.

I. INTRODUCTION

Nuclear fission poses a challenging quantum many-body problem. It is intrinsically nonperturbative. Although it involves classical liquid drop physics through the competition of surface and Coulomb energies, tunneling in the classically forbidden regime must ultimately be understood in a consistent quantum theory. Furthermore, it involves the delicate interplay of collective and single-particle degrees of freedom.

Functional integrals provide a natural and powerful framework in which to understand and systematically approximate spontaneous fission.[1-5] Starting with an exact representation of the evolution operator, the stationary-phase approximation specifies the dominant path in the space of all Slater determinants for evolution of the metastable parent state through the barrier to the final fission fragments. The theory is thus fully microscopic and consistently combines liquid drop behavior and single-particle shell effects. The trajectory in the space of Slater determinants is determined by self-consistent mean-field equations and thus does not require any *ansatz* for the fission path as in constrained Hartree-Fock or generator-coordinate treatments. Finally, since the theory is based on the stationary-phase approximation to an exact functional integral, it is amenable to systematic corrections.

The principal impediment in applying this theory to heavy nuclei is the practical difficulty in solving the periodic mean-field equations. Hence, the purpose of the present work is to present a general new technique which is applicable in four space-time dimensions with a large number of occupied states. The basic idea of applying a filter to iteratively refine an initial approximation has its roots in familiar methods which have been applied to the static Hartree-Fock equations. Here, we present a general formulation of the filter method, analyze its stability and convergence, and generalize it to address unique aspects of the nuclear fission problem.

The outline of the paper is as follows. In Sec. II we review the mean-field theory for spontaneous decay, and in Sec. III we present the general filter method in the special case of the static Hartree equations. Although the generalization to include exchange terms is obvious and straightforward, for simplicity, throughout this work, we will suppress exchange terms and treat only the direct Hartree potential. The periodic mean field equations in imaginary time are addressed in Sec. IV. The pathologies associated with naive time discretization are identified and circumvented by exact time evolution in a piecewise continuous potential and the generalized filter method is applied. Much of the structure of the general solutions may be elucidated by the study of solutions in the vicinity of the saddle point, and this special case is addressed in Sec. V. The last section applies the filter method to a self-consistent fission problem.

II. MEAN-FIELD THEORY OF SPONTANEOUS FISSION

The mean-field theory for spontaneous fission is obtained by applying the stationary-phase approximation to an exact functional integral for the density of states[1] or transition matrix element between the metastable parent nucleus and fission fragments.[2] Depending on the form of auxiliary field which is introduced or the use of a path integral in the space of Slater determinants, the mean field equations either include a local Hartree field or a nonlocal Hartree-Fock field. Since the presence of exchange terms does not affect the method of solution discussed here, we simplify the notation and discussion by treating the Hartree case.

The path which dominates spontaneous decay is specified by the periodic self-consistent solution to the following eigenvalue problem:

$$\left[\frac{\partial}{\partial \tau} + \hat{h}_\sigma(\mathbf{x},t) \right] \phi_\alpha(\mathbf{x},\tau) = \lambda_\alpha \phi_\alpha(\mathbf{x},\tau) , \tag{2.1}$$

where the single-particle Hamiltonian is defined as

$$\hat{h}_\sigma(\mathbf{x},\tau) = T + \int d\mathbf{x}' v(\mathbf{x}-\mathbf{x}')\sigma(\mathbf{x}',\tau) , \tag{2.2}$$

the σ field, which corresponds to the physical density, is given by

$$\sigma(\mathbf{x},\tau) = \sum_\alpha \phi_\alpha(\mathbf{x}, -\tau)\phi_\alpha(\mathbf{x},\tau) , \tag{2.3}$$

the sum over α includes the N states with the lowest real eigenvalue λ_α, the kinetic energy operator is written

$$T = -\frac{\hbar^2}{2m}\nabla_x^2 \ , \tag{2.4}$$

and the single-particle wave functions satisfy the periodic boundary condition

$$\phi_\alpha\left[\mathbf{x},\frac{T}{2}\right] = \phi_\alpha\left[\mathbf{x},-\frac{T}{2}\right] \tag{2.5}$$

and the orthonormality condition

$$\int d\mathbf{x}\,\phi_\alpha(\mathbf{x},-\tau)\phi_\beta(\mathbf{x},\tau) = \delta_{\alpha\beta} \ . \tag{2.6}$$

In the limit in which $T \to \infty$, this period solution approaches the so-called bounce solution which evolves from the Hartree ground state, through the fission barrier to the classically allowed regime. The lifetime is given by the sum over the bounces to all the possible fission channels a,

$$\Gamma = \lim_{T\to\infty} \sum_a \kappa_{(a)}\exp\left[-\int_{-T/2}^{T/2} d\tau \int d\mathbf{x} \sum_\alpha \phi_\alpha^{(a)}(\mathbf{x},-\tau)\frac{\partial}{\partial\tau}\phi_\alpha^{(a)}(\mathbf{x},\tau)\right] \ . \tag{2.7}$$

The premultiplying factor $\kappa_{(a)}$ may be written in terms of the determinant of the second derivative of the action, but its evaluation is beyond the scope of the present work.

As discussed in Refs. 1, 3, and 4, the structure of this theory is analogous to tunneling of a single particle in a potential. The stationary solution in the classically forbidden region corresponds to evolution in purely imaginary time, in which case the equation of motion with t replaced by $-i\tau$ corresponds to the classical equation of motion in the inverted potential. In the many-fermion problem, the time dependent Hartree-Fock equations have Hamiltonian form with $\phi^*(\mathbf{x},\tau)$ and $\phi(\mathbf{x},t)$ playing the role of canonical variables p and q in real time which become $\phi(\mathbf{x},-\tau)$ and $\phi(\mathbf{x},\tau)$ in imaginary time. Equation (2.1) may be thought of as time-dependent Hartree equations in an inverted potential[1] and the exponent in Eq. (2.6) is analogous to the familiar form $\int p\,dq$. Note that whereas this description of evolution in imaginary time provides a very picturesque way to visualize the sequence of configurations along the fission path, the imaginary time variable τ has no direct relation to the fission lifetime. Ultimately, τ is simply a continuous parameter which has been broken up into infinitesimal slices to handle the noncommutativity of the kinetic and potential terms in the Hamiltonian.

For subsequent developments, it is useful to rewrite the basis equations (2.1)–(2.5) in an equivalent alternative form. We define

$$\phi_\alpha(\mathbf{x},\tau) = e^{\lambda_\alpha(\tau + T/2)}\psi_\alpha(\mathbf{x},\tau) \ , \tag{2.8}$$

so that the equation of motion (2.1) takes on the time-dependent Hartree form

$$\left[\frac{\partial}{\partial\tau} + \hat{h}(\mathbf{x},\tau)\right]\psi_\alpha(\mathbf{x},\tau) = 0 \tag{2.9}$$

with the quasiperiodic boundary condition

$$\psi_\alpha\left[\mathbf{x},\frac{T}{2}\right] = e^{-\lambda_\alpha T}\psi_\alpha\left[\mathbf{x},-\frac{T}{2}\right] \ , \tag{2.10}$$

and the mean field is

$$\sigma(\mathbf{x},\tau) = \sum_\alpha \frac{\psi_\alpha(\mathbf{x},-\tau)\psi_\alpha(\mathbf{x},\tau)}{\int d\mathbf{x}\,\psi_\alpha(\mathbf{x},-\tau)\psi_\alpha(\mathbf{x},\tau)} \ . \tag{2.11}$$

Also, it is convenient to define the evolution operator for the equation of motion (2.9),

$$U_\sigma(\tau_f,\tau_i) = T\exp\left[-\int_{T_i}^{T_f} d\tau\,\hat{h}_\sigma(\mathbf{x},\tau)\right] \ , \tag{2.12}$$

where T denotes the time-ordering operator. The wave functions $\psi_\alpha(\mathbf{x},\tau)$ may then be written

$$\psi_\alpha(\mathbf{x},\tau) = U_\sigma\left[\tau,-\frac{T}{2}\right]\psi_\alpha\left[\mathbf{x},-\frac{T}{2}\right] \ , \tag{2.13}$$

and the wave functions at $-T/2$ are specified by the spatial eigenvalue problem

$$U_\sigma\left[\frac{T}{2},-\frac{T}{2}\right]\psi_\alpha\left[\mathbf{x},-\frac{T}{2}\right] = e^{-\lambda_\alpha T}\psi_\alpha\left[\mathbf{x},-\frac{T}{2}\right]$$

$$\equiv \Lambda_0\psi_\alpha\left[\mathbf{x},-\frac{T}{2}\right] \ . \tag{2.14}$$

We will consider only real wave functions and time-even $\sigma(\mathbf{x},\tau)$, in which case $U_\sigma(T/2,-T/2)$ is real and symmetric and has real eigenvalues Λ_α. Note that this restriction is self-consistent: by Eq. (2.11), real wave functions produce a real, time-even $\sigma(x,\tau)$ and the Hermitian eigenvalue problem (2.14) has real eigenfunctions from which purely real wave functions $\psi_\alpha(x,\tau)$ are obtained using (2.13).

In addition to being real, the eigenvalues Λ_α are positive, as seen by the following argument. For time-even $\sigma(\tau)$, Eq. (2.12) implies

$$U_\sigma\left[\frac{T}{2},0\right]^\dagger = U_\sigma\left[0,-\frac{T}{2}\right] \ . \tag{2.15}$$

If we denote the eigenvectors of the spatial operator $U_\sigma(T/2,-T/2)$ as

$$\chi_\alpha(\mathbf{x}) = \psi_\alpha\left[\mathbf{x},-\frac{T}{2}\right] \equiv \phi_\alpha\left[\mathbf{x},-\frac{T}{2}\right] \ ,$$

which satisfy

$$U_\sigma\left[\frac{T}{2},-\frac{T}{2}\right]\chi_\alpha = \Lambda_\alpha\chi_\alpha \ , \tag{2.16}$$

and expand an arbitrary function in these eigenvectors,

$$f(\mathbf{x}) = \sum_\alpha f_\alpha \mathcal{X}_\alpha(\mathbf{x}) , \tag{2.17}$$

then

$$\left\langle f \left| U\left[\frac{T}{2}, -\frac{T}{2}\right] \right| \right\rangle = \sum_\alpha f_\alpha^2 \Lambda_\alpha$$

$$= \left\langle f \left| U\left[0, -\frac{T}{2}\right]^\dagger U\left[0, -\frac{T}{2}\right] \right| f \right\rangle$$

$$= \left| U\left[0, -\frac{T}{2}\right] | f \rangle \right|^2$$

$$> 0 . \tag{2.18}$$

Hence, since the expansion coefficients f_α are arbitrary, each of the eigenvalues Λ_α is positive.

In terms of the eigenfunctions $\mathcal{X}_\alpha(\mathbf{x})$ of the spatial eigenvalue problem (2.16) with a known σ, the bounce solution is specified as follows. The N eigenfunctions $\mathcal{X}_\alpha(\mathbf{x})$ with the largest eigenvalues Λ_α define the single-particle wave functions at time $\tau = -T/2$, $\psi_a(\mathbf{x}, -T/2)$. The N single-particle wave functions at general time τ, $\psi_\alpha(\mathbf{x},\tau)$, are then given by the solution of the time-dependent Hartree initial-value problem, Eq. (2.9). Self-consistency requires that $\sigma(\mathbf{x},\tau)$ obtained from these wave functions using (2.11) agrees with the original σ in $\hat{h}_\sigma$ and is obtained, in practice, using some form of iterative algorithm.

Having understood the structure of the solutions to the spatial eigenvalue problem, Eq. (2.16), it is useful to consider the structure of the associated space-time eigenvalue problem, Eq. (2.1). Since the operator in (2.1) has one additional time dimension relative to the operator in (2.16), it has more eigenfunctions and it is useful to label each

eigenfunction by a spatial label α and a temporal label n. Thus, we rewrite Eq. (2.1) in the form

$$\left[\frac{\partial}{\partial\tau} + \hat{h}_\sigma(\mathbf{x},\tau)\right]\phi_{\alpha,n}(\mathbf{x},\tau) = \lambda_{\alpha n}\phi_{\alpha,n}(\mathbf{x},\tau) . \tag{2.19}$$

Let us first denote by the label $n=0$ the set of eigenfunctions with real eigenvalues $\lambda_{\alpha 0}$ defined by

$$e^{-\lambda_{\alpha 0} T} = \Lambda_\alpha . \tag{2.20}$$

Since we have proved above that each Λ_α is positive, there always exists one real $\lambda_{\alpha 0}$ satisfying Eq. (2.20). It then follows from Eq. (2.8) that the real function

$$\phi_{\alpha 0}(\mathbf{x},\tau) = e^{\lambda_{\alpha 0}(\tau + T/2)}\psi_\alpha(\mathbf{x},\tau) \tag{2.21}$$

is an eigenvector of (2.19) with eigenvalue $\lambda_{\alpha 0}$.

In addition to these real solutions with real eigenvalues, there is an infinite set of complex solutions defined by an integer n,

$$\phi_{\alpha n}(\mathbf{x},\tau) = e^{i(2\pi n/T)\tau}\phi_{\alpha 0}(\mathbf{x},\tau) , \tag{2.22}$$

$$\lambda_{\alpha n} = \lambda_{\alpha 0} + i\frac{2\pi n}{T} . \tag{2.23}$$

We will refer to all the states with the same α and different n as members of the same family, and refer to the real solutions $\phi_{\alpha 0}(\mathbf{x},\tau)$ as the fundamental solutions for that family. Note that different eigenfunctions within a family differ only by trivial time-dependent phase factors and that the combination $\phi_{\alpha n}(\mathbf{x}, -\tau)\phi_{\alpha n}(\mathbf{x},\tau)$ contributing to σ is the same for every member of a given family.

The orthonormality properties of the eigenfunctions follow from Eq. (2.19). For two arbitrary states $\phi_{\alpha n}(\mathbf{x},\tau)\phi_{\beta m}(\mathbf{x},\tau)$,

$$\frac{d}{d\tau}\int d\mathbf{x}\,\phi_{\alpha n}(\mathbf{x}, -\tau)\phi_{\beta m}(\mathbf{x},\tau) = (\lambda_{\beta m} - \lambda_{\alpha n})\int d\mathbf{x}\,\phi_{\alpha n}(\mathbf{x}, -\tau)\phi_{\beta m}(\mathbf{x},\tau) , \tag{2.24}$$

so that

$$\int d\mathbf{x}\,\phi_{\alpha n}(\mathbf{x}, -\tau)\phi_{\beta m}(\mathbf{x},\tau) = e^{(\lambda_{\beta m} - \lambda_{\alpha n})(\tau + T/2)}\int d\mathbf{x}\,\phi_{\alpha n}\left[\mathbf{x}, \frac{T}{2}\right]\phi_{\beta m}\left[\mathbf{x}, -\frac{T}{2}\right] . \tag{2.25}$$

Hence, if two states are orthogonal at any time, they are orthogonal at all times. Furthermore, evaluating (2.25) at $\tau = T/2$ and using the periodicity of ϕ, two states are nonorthogonal only if $\lambda_{\beta m} - \lambda_{\alpha n}$ is an integer multiple of $2\pi i/T$; that is, they belong to the same family.

So far we have considered the space-time continuum. In practical calculations, it is desirable to define the problem on a space-time lattice and approximate the continuum limit using a small lattice spacing. We then define wave functions on lattice sites $\phi_{n\alpha}(\mathbf{x}_j, \tau_i)$ with $j = 1, \ldots, N_x$ and $i = 1, \ldots, N_\tau$. Here, N_τ denotes the number of time slices and N_x denotes the total number of spatial mesh points and there is no loss of generality in labeling the spatial coordinates in any number of dimensions with a single integer j.

The obvious way to define the analog of the continuum

theory on the spatial lattice is to replace the continuum kinetic energy operator $-(\hbar^2/2m)\nabla^2$ by a finite difference operator. At a given time, the spatial operator $\hat{h}_\sigma(\mathbf{x})$ is thus replaced by a sparse matrix which connects the wave function at site $\mathbf{x}_j$ with neighboring sites in each of the spatial directions.

In contrast, there are two rather different options for treatment of the time variable. One possibility implemented in Ref. 1 is to replace $\partial/\partial\tau$ in Eq. (2.19) by a difference formula analogous to the treatment of the spatial derivatives, in which case $\partial/\partial\tau + \hat{h}_\sigma(\mathbf{x},\tau)$ is replaced by a sparse matrix of dimension $N_\tau \times N_x$. The bounce solution is then given by the N real eigenvectors of this matrix with the lowest real eigenvalues. As discussed in detail in Sec. IV, however, different solutions in the same

family do not satisfy the continuum relations (2.22) and (2.23). In particular, family members do not differ from the fundamental member by a multiplicative factor, and their eigenvalues do not have the same real part. We will see that these features cause serious difficulties in systems with a large number of occupied states.

The second option for treating the time is to define the evolution operator, or transfer matrix, between adjacent time slices as

$$U(\tau_{i+1},\tau_i) \equiv e^{-\Delta\tau \hat{h}[\sigma(t_{i+1/2})]} , \tag{2.26}$$

where the average density between time slices is

$$\sigma(\mathbf{x}_j,\tau_{i+1/2}) = \tfrac{1}{2}[\sigma(\mathbf{x}_j,\tau_i)+\sigma(\mathbf{x}_j,\tau_{i+1})] . \tag{2.27}$$

This definition is equivalent to solving the continuum time equations with the piecewise-continuous density

$$\sigma(\mathbf{x}_j,\tau) = \sum_i \Theta(\tau-\tau_i)\Theta(\tau_{i+1}-\tau)\sigma(\mathbf{x}_j,\tau_{i+1/2}) . \tag{2.28}$$

For symmetrically placed time slices, this density will be time even, the evolution operator $U(T/2, -T/2)$ will be Hermitian with positive eigenvalues as before, and the eigenfunctions of the space-time eigenvalue problem (2.19) will satisfy Eqs. (2.22) and (2.23). These properties are essential for the method of solution presented in Sec. IV for the solution of large, realistic fission problems in which the dimensionality of the matrices appearing in the eigenvalue problem precludes straightforward diagonalization.

III. FILTER METHOD FOR THE STATIC HARTREE EQUATIONS

Although the ultimate objective of this work is to solve the periodic self-consistent time-dependent Hartree equations, Eqs. (2.1)—(2.5), the essential ideas may be illustrated most closely for the structurally similar but more familiar static Hartree equations. In this section, we will therefore describe the general iterative filter method as it applies to the static Hartree problem, show the relation between the physical stability of the Hartree ground state and convergence of the filter iterations, and discuss the treatment of constraints.

Nonlinear self-consistent problems such as the static Hartree equations are solved by iteration. In the general case, one defines a functional specifying the $(n+1)$th set of wave functions $\{\phi_k^{(n+1)}(x)\}$ from a previous set of wave functions $\{\phi_k^{(n)}(x)\}$,

$$\phi^{(n+1)} = F[\phi^{(n)}] , \tag{3.1}$$

and seeks convergence to a fixed point

$$\phi^* = F[\phi^*] , \tag{3.2}$$

at which point self-consistency is achieved. The familiar Hartree iteration procedure, evolution in imaginary time, and the Lanczos method, are examples of different functionals used in practical calculations.

Iterative maps have been extensively studied in connection with problems ranging from chaos to the renormalization group. Even simple one-dimensional maps show

rich structure. In some regions of parameter space, a sequence of variables x^n always converges to a single stable fixed point. In other cases there may be both stable and unstable fixed points with separate basins of attraction leading to different stable fixed points. The map may not converge to a single fixed point, but rather approach an n-point limit cycle or yield a totally chaotic sequence. For the general case of functional iteration, (3.1), it is not possible to analyze the general global structure, and we will restrict our attention to the structure of the map in the vicinity of the fixed point corresponding to the desired physical solution, in which case it can be expanded around the fixed point and its stability and convergence can be analyzed.

A. Filter method for the Schrödinger equation

Consider first the problem of finding the lowest A eigenfunctions of the Schrödinger equation

$$\hat{h}\phi_k = \left[-\frac{\hbar^2}{2m}\nabla_x^2 + V(\mathbf{x}) \right]\phi_k = \epsilon_k\phi_k . \tag{3.3}$$

To establish contact with the subsequent Hartree problem in which we consider A occupied or hole states and regard all other states as unoccupied or particle states, we will use the convention that the indices i,j,k,l run from 1 to A and denote the A lowest eigenstates and the indices p,q,r,s run from $A+1$ to ∞ and denote the higher eigenstates. The indices a,b,c,d will run from 1 to ∞.

The filter functional specifying the $(n+1)$st set of A wave function $\{\phi_k^{(n+1)}(\mathbf{x})\}$ in terms of the nth iteration $\{\phi_k^n(\mathbf{x})\}$ may be written schematically as follows:

$$\phi_k^{(n+1)} = \mathscr{O}f(\hat{h})\phi_k^{(n)} , \tag{3.4}$$

where f is a fixed function we will refer to as the filter and $\mathscr{O}$ denotes Graham-Schmidt orthogonalization. Specifically, we consider $f(\hat{h})$ defined as a Taylor series or finite polynomial and construct the intermediate set $\bar{\phi}_k^{(n+1)} = f(\hat{h})\phi_k^{(n)}$ for $1 \le k \le A$. The set $\{\phi_k^{(n+1)}\}$ is then constructed from the set $\{\bar{\phi}_k^{(n+1)}\}$ by Graham-Schmidt orthonormalization, beginning with the state $k=1$ and proceeding with increasing k.

To understand the method and the criteria for selecting f, it is instructive to analyze the iteration in the neighborhood of the fixed point. We assume the set $\{\phi_k^{(n)}\}$ is close to the exact solutions $\{\phi_k\}$, where the states are labeled in order of increasing eigenvalues, and define

$$\phi_k^{(n)} = \sum_{a=1}^{\infty} C_{ka}^{(n)}\phi_a . \tag{3.5}$$

In Appendix A, we show

$$\phi_k^{(n+1)} = \phi_k + \sum_{j=1}^{k-1} C_{kj}^{(n)}\frac{f(\epsilon_k)}{f(\epsilon_j)}\phi_j + \sum_{p=k+1}^{\infty} C_{kp}^{(n)}\frac{f(\epsilon_p)}{f(\epsilon_k)}\phi_p . \tag{3.6}$$

Therefore if

$$\left| \frac{f(\epsilon_k)}{f(\epsilon_j)} \right| < 1, \quad j < k \le A \tag{3.7}$$

and

$$\left| \frac{f(\epsilon_p)}{f(\epsilon_k)} \right| < 1, \quad k \leq A, \, p > A \tag{3.8}$$

then $\phi_k^{(n+1)} \rightarrow \phi_k$ as $n \rightarrow \infty$ for all $k \leq A$. From Eqs. (3.7) and (3.8), an effective filter must decrease monotonically for the range of energies $\epsilon_1, \epsilon_2, \ldots, \epsilon_a$ (which will correspond to hole states in the many-body problem) and be larger in this region of energies than in the region of energies $\epsilon_p > \epsilon_A$ (corresponding to particle states in the many-body problem). The rate of convergence is given by the relations

$$C_{ka}^{(n+1)} = C_{ka}^{(n)} \frac{f(\epsilon_a)}{f(\epsilon k)} \quad (a > k) . \tag{3.9}$$

Note that this filter method fails if any of the hole states are degenerate or nearly degenerate with each other or with the lowest particle states. If such degeneracies occur, the method must be modified by diagonalizing h in the degenerate subspace.

In applications of practical interest, $\hat{h}$ will be represented by a sparse differrence matrix in coordinate space for which matrix multiplication of a column vector $\psi(\mathbf{x}_i)$ by $h(\mathbf{x}_i, \mathbf{x}_j)$ will be easy and efficient to perform. Hence, $f(\hat{h})$ will be chosen to be a polynomial or truncated power series expansion. Since any polynomial $f(\epsilon)$ blows up as $\epsilon \rightarrow \infty$, we must use the fact that the lattice defines a cutoff ϵ_{max} on the maximum eigenvalue of $h(\mathbf{x}_i, \mathbf{x}_j)$ and choose the filter so that condition (3.8) is satisfied for all $\epsilon_p \leq \epsilon_{max}$.

We may estimate ϵ_{max} by calculating the highest eigenvalue of the discrete lattice kinetic energy operator. For example, the five-point approximation to the second derivative in one dimension yields the eigenvalue problem

$$\frac{\hbar^2}{24m(\Delta x)^2}(\psi_{n-2} - 16\psi_{n-1} + 30\psi_n - 16\psi_{n+1} + \psi_{n-2})$$

$$= \epsilon\psi_n \tag{3.10}$$

with eigenvectors

$$\psi_n = e^{i\alpha n}, \quad \alpha = \frac{2\pi}{N}m, \quad -\frac{N}{2} \leq m \leq \frac{N}{2} \tag{3.11}$$

and eigenvalues

$$\epsilon_m = \frac{\hbar^2}{12m(\Delta x)^2}(\cos 2\alpha - 16\cos\alpha - 15) . \tag{3.12}$$

The maximum eigenvalue occurs for the mode with $\alpha = \pm\pi$, which we call the sawtooth mode because it alternates in sign at each lattice site. The energy of the sawtooth mode is

$$\epsilon_{max} = \frac{8\hbar^2}{3m(\Delta x)^2} . \tag{3.13}$$

Note that this energy increases as $1/(\Delta x)^2$, so that as one approaches a more accurate description of the continuum, the lattice can support higher Fourier components and the filter must be capable of damping higher energy modes. For small Δx, the kinetic energy of the sawtooth mode dominates any potential energy relevant to a single nu-

cleon wave function, and we may use Eq. (3.13) (or its counterpart in d space dimension, or for alternative finite difference approximations) as an estimate of the maximum lattice eigenvalue. In the following discussion of filters, we will assume that the Hamiltonian $\hat{h}$ has been shifted and scaled such that all its eigenvalues lie between 0 and ϵ_{max} and that ϵ_{max} is large compared to the A lowest eigenvalues of physical interest.

Several examples of filters satisfying the properties (3.7) and (3.8) are shown in Fig. 1. One natural choice for a filter is the exponential $f(\hat{h}) = e^{-\beta\hat{h}}$, which is used when the Schrödinger equation or Hartree-Fock equations are solved by evolution in imaginary time. Since it is monotonically decreasing, it obviously satisfies the requirements (3.7) and (3.8). In practice, however, the exact exponential must be approximated by a polynomial. One option is a truncated Taylor series

$$e^{-\beta\hat{h}} \approx f(\hat{h}) \equiv \sum_{n=0}^{N} \frac{-(\beta\hat{h})^n}{n!} . \tag{3.14}$$

For large N, the criterion that $|f(\epsilon_{max})| < 1$ implies $\beta\epsilon_{max}/N! \lesssim 1$, so that using Stirling's approximation we require $N > \beta e \epsilon_{max}$. The solid curve in Fig. 1 shows a seven-term Taylor expansion with β defined such that $|f(\epsilon_{max})| = 0.9$.

A second approximation to the exponential is the Napier approximation

$$e^{-\beta\hat{h}} \approx f(\hat{h}) \equiv \left[1 - \frac{\beta}{N}\hat{h}\right]^N . \tag{3.15}$$
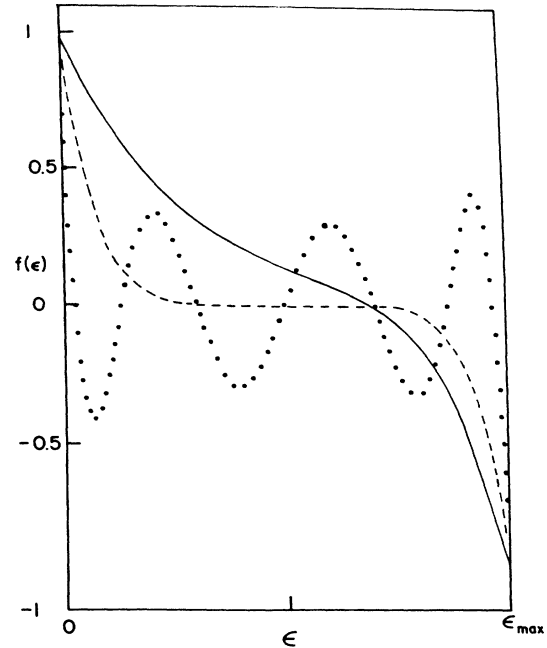

FIG. 1. Alternative polynomial filters of seventh degree. The solid line is a seven-term Taylor expansion of an exponential, the dashed line is a seven-term Napier approximation to an exponential, and the dotted curve is a Legendre polynomial $P_7(\epsilon)$. In each case, the argument is scaled such that $|f(\epsilon_{max})| = 0.9$.

In this case, the criterion $f(\epsilon_{\max}) < 1$ is satisfied if $N < \beta\epsilon_{\max}/2$, which is a factor $1/2e$ smaller than for the Taylor series. That is, for a given β, the Taylor expansion requires 5.44 times as many terms to avoid contamination from the sawtooth mode or, for a fixed N, the Napier approximation can refine the physical low eigenvalues with a β which is 5.44 times larger. The dashed line in Fig. 1 shows the superiority of the Napier formula as a filter for the case of seven terms.

An even better seventh order polynomial filter from the viewpoint of convergence is the Legendre polynomial

$$f(\hat{h}) = P_N \left[1 - \frac{2\hat{h}}{\epsilon_{\max}} \right] , \qquad (3.16)$$

shown by the dotted line in Fig. 1. The slope at the origin is even steeper than either of the approximations to the exponential, giving rise to more rapid refinement of the physical low eigenvalues, and yet $|f(\epsilon)| < 1$ below $\epsilon_{\max}$.

For the applications of interest, in which the relevant eigenvalues are very small compared with $\epsilon_{\max}$, the rate of convergence is governed by the slope at $\epsilon \sim 0$. This is seen by writing the convergence criterion (3.9) for small ϵ_a and ϵ_k,

$$\frac{f(\epsilon_a)}{f(\epsilon_k)} \simeq 1 + (\epsilon_a - \epsilon_k)\frac{f'(0)}{f(0)} . \qquad (3.17)$$

Thus, the optimal polynomial of degree N is that for which $f(0) = 1$, $|f(\epsilon)| < 1$, for $0 < \epsilon \le \epsilon_{\max}$, and $f'(0)$ is minimized. Whereas we have not succeeded in proving that Legendre polynomials are optimal in this sense, they are the best polynomials we have found and are much superior to the two approximations to the exponential discussed above. In fact, using the property of Legendre polynomials

$$\frac{d}{dx}P_N(x)\bigg|_{x=-1} = \frac{N(N+1)}{2}P_N(-1) ,$$

we may compare the slopes of the three filters (3.14)–(3.16) with polynomials of degree N as follows:

$$\frac{f'(0)}{f(0)} = \frac{-N}{\epsilon_{\max}} \times \begin{cases} 1/e, & \text{Taylor series} , \\ 2, & \text{Napier formula} , \\ N+1, & \text{Legendre polynomial} . \end{cases} \qquad (3.18)$$

B. Filter method for the static Hartree equations

We now address the problem of self-consistency by replacing the fixed potential $V(\mathbf{x})$ in the linear Schrödinger equation with the self-consistent Hartree potential. To show that the method is also applicable to density-dependent effective interactions, we will consider the case in which the single-particle Hamiltonian contains a density-dependent δ function interaction,[6]

$$\hat{h}[\phi]\phi_k = \left[-\nabla_x^2 + \int dy\, v(\mathbf{x}-\mathbf{y})\rho(\mathbf{y}) + V_\delta\rho^2(\mathbf{x}) \right]\phi_k = \epsilon_k\phi_k , \qquad (3.19)$$

$$\rho(\mathbf{x}) = M \sum_{k=1}^{A} \phi_k^*(\mathbf{x})\phi_k(\mathbf{x}) ,$$

where M is the spin-isospin degeneracy and A is the number of occupied single-particle states. Although the method also applies when exchange terms and finite-range density dependent interactions are included, these terms are omitted from the present discussion to simplify the presentation.

The filter functional is written schematically as follows:

$$\phi_k^{(n+1)} = \mathcal{O}f(\hat{h}[\phi^{(n)}])\phi_k^{(n)} . \qquad (3.20)$$

Explicitly, given the single-particle wave functions $\{\phi_k^{(n)}(\mathbf{x})\}$, one constructs the density

$$\rho^{(n)}(\mathbf{x}) = M \sum_k \phi_k^{(n)*}(\mathbf{x})\phi_k^{(n)}(\mathbf{x}) ,$$

which specifies the Hamiltonians

$$\hat{h}^{(n)} = -\nabla_x^2 + \int dy\, v(\mathbf{x}-\mathbf{y})\rho^{(n)}(\mathbf{y}) + V_\delta\rho^{(n)2}(\mathbf{x}) .$$

One then constructs the intermediate set $\bar{\phi}_k^{(n+1)} = f(\hat{h}^{(n)})\phi_k^{(n)}$ and the set $\{\phi_l^{(n+1)}\}$ is obtained from the set $\{\bar{\phi}_k^{(n+1)}\}$ by the Graham-Schmidt orthogonalization.

As for the linear Schrödinger equation, we shall analyze the effect of one iteration in the vicinity of a fixed point. For the present, we will consider general complex wave functions and later restrict our attention to the real domain. We again assume that the set $\{\phi_k^{(n)}\}$ is close to the set of eigenfunctions $\{\phi_k\}$ and expand

$$\phi_k^{(n)} = \sum_{j=1}^{A} C_{kj}^{(n)}\phi_j + \sum_{p>A} C_{kp}^{(n)}\phi_p . \qquad (3.21)$$

As in the preceding subsection, we will use the indices ranging from $A+1$ to ∞ and the indices a,b,c,d to denote all states ranging from 1 to ∞. Since the set $\{\phi_k^{(n)}\}$ is orthogonal, $\{C_{kj}^{(n)}\}_{k,j=1,2,\ldots,A}$ is unitary and we may write

$$C_{kj}^{(n)} = \delta_{kj} + i\epsilon_{kj}^{(n)}, \quad \epsilon_{kj}^{(n)*} = \epsilon_{jk}^{(n)} , \qquad (3.22)$$

where the ϵ_{ij} are assumed to be small. The coefficient $C_{kk}^{(n)}$ is an irrelevant phase which may be removed. The density at iteration n is

$$\rho^{(n)} = M \sum_{k=1}^{A} \phi_k^{(n)*}\phi_k^{(n)}$$
$$= \rho + M \sum_{kp}(C_{kp}^{(n)}\phi_k^*\phi_p + C_{kp}^{(n)*}\phi_k\phi_p^*) . \qquad (3.23)$$

The potential may be written

$$V^{(n)}(\mathbf{x}) = \int dy\, \rho^{(n)}(\mathbf{y})v(\mathbf{x}-\mathbf{y}) + V_\delta\rho^{(n)2}(\mathbf{x})$$
$$\equiv V(\mathbf{x}) + \delta V^{(n)}(\mathbf{x}) , \qquad (3.24)$$

where

$$\delta V^{(n)}(\mathbf{x}) = M \sum_{ka}[C_{ka}^{(n)}V_{ka}(\mathbf{x}) + C_{ka}^{(n)*}V_{ak}(\mathbf{x})] \qquad (3.25)$$

and

$$V_{ka}(\mathbf{x}) = \int dy\, \phi_k^*(\mathbf{y})[v(\mathbf{x}-\mathbf{y}) + 2V_\delta\rho(\mathbf{x})\delta(\mathbf{x}-\mathbf{y})]\phi_a(\mathbf{y}) . \qquad (3.26)$$

We define

$$\bar{\phi}_k^{(n+1)} = f(\hat{h}^{(n)})\phi_k^{(n)} = \sum_{a=1}^{\infty} \mathscr{C}_{ka}\phi_a \ , \qquad (3.27)$$

and it is shown in Appendix B that the coefficients $\mathscr{C}_{ka}$ are

$$\mathscr{C}_{kk} = f(\epsilon_k) + f'(\epsilon_k)\langle k \mid \delta V^{(n)} \mid k \rangle \ ,$$

$$\mathscr{C}_{kj} = f(\epsilon_j)C_{kj}^{(n)} + \frac{f(\epsilon_k) - f(\epsilon_j)}{\epsilon_k - \epsilon_j}\langle j \mid \delta V^{(n)} \mid k \rangle \ , \qquad (3.28)$$

$$\mathscr{C}_{kp} = f(\epsilon_p)C_{kp}^{(n)} + \frac{f(\epsilon_p) - f(\epsilon_k)}{\epsilon_p - \epsilon_k}\langle p \mid \delta V^{(n)} \mid k \rangle \ .$$

Graham-Schmidt orthogonalization of the set $\{\bar{\phi}_k^{(n+1)}\}$ then yields, after some algebra, the result

$$C_{kp}^{(n+1)} = \frac{\mathscr{C}_{kp}}{\mathscr{C}_{kk}} \ ,$$

$$C_{kj}^{(n+1)} = \frac{\mathscr{C}_{kj}}{\mathscr{C}_{kk}} \quad (j > k) \ , \qquad (3.29)$$

$$C_{kj}^{(n+1)} = -\frac{\mathscr{C}_{jk}^*}{\mathscr{C}_{jj}} \quad (j < k) \ .$$

Therefore,

$$C_{kp}^{(n+1)} = \frac{f(\epsilon_p)}{f(\epsilon_k)}C_{kp}^{(n)} + \frac{f(\epsilon_p)/f(\epsilon_k) - 1}{\epsilon_p - \epsilon_k}M\sum_{iq}(C_{iq}^{(n)}\langle p \mid V_{iq} \mid k \rangle + C_{iq}^{(n)*}\langle p \mid V_{qi} \mid k \rangle) \ ,$$

$$C_{kj}^{(n+1)} = \frac{f(\epsilon_j)}{f(\epsilon_k)}C_{kj}^{(n)} + \frac{f(\epsilon_j)/f(\epsilon_k) - 1}{\epsilon_j - \epsilon_k}M\sum_{iq}(C_{iq}^{(n)}\langle j \mid V_{iq} \mid k \rangle + C_{iq}^{(n)*}\langle j \mid V_{qi} \mid k \rangle) \quad (k < j) \ , \qquad (3.30)$$

$$C_{kj}^{(n+1)} = -\frac{f(\epsilon_k)}{f(\epsilon_j)}C_{jk}^{(n)*} = \frac{f(\epsilon_k)/f(\epsilon_j) - 1}{\epsilon_k - \epsilon_j}M\sum_{iq}(C_{iq}^{(n)}\langle j \mid V_{iq} \mid k \rangle + C_{iq}^{(n)*}\langle j \mid V_{qi} \mid k \rangle) \quad (k > j) \ .$$

The expansion coefficients $C^{(n+1)}$ are then related to the coefficients $C^{(n)}$ by the following stability matrix:

$$\begin{bmatrix} C_{k,j<k}^{(n+1)} \\ C_{k,j<k}^{(n+1)*} \\ C_{k,j>k}^{(n+1)} \\ C_{k,j>k}^{(n+1)*} \\ C_{kp}^{(n+1)} \\ C_{kp}^{(n+1)*} \end{bmatrix} = \begin{bmatrix} L & 0 & 0 & 0 & P & \tilde{P} \\ 0 & L & 0 & 0 & \tilde{P}^* & P^* \\ 0 & 0 & L & 0 & P & \tilde{P} \\ 0 & 0 & 0 & L & \tilde{P}^* & P^* \\ 0 & 0 & 0 & 0 & S & T \\ 0 & 0 & 0 & 0 & T^* & S^* \end{bmatrix} \begin{bmatrix} C_{k,j<k}^{(n)} \\ C_{k,j<k}^{(n)*} \\ C_{k,j>k}^{(n)} \\ C_{k,j>k}^{(n)*} \\ C_{kp}^{(n)} \\ C_{kp}^{(n)*} \end{bmatrix} \ ,$$

$$(3.31)$$

where

$$L_{kj,ih} = \delta_{ki}\delta_{jh}\frac{f(\epsilon_>)}{f(\epsilon_<)} \ ,$$

$$S_{kp,iq} = \delta_{ki}\delta_{pq}\frac{f(\epsilon_p)}{f(\epsilon_k)} + \frac{f(\epsilon_p)/f(\epsilon_k) - 1}{\epsilon_p - \epsilon_k}M\langle p \mid V_{iq} \mid k \rangle \ ,$$

$$T_{kp,iq} = \frac{f(\epsilon_p)/f(\epsilon_k) - 1}{\epsilon_p - \epsilon_k}M\langle p \mid V_{qi} \mid k \rangle \ , \qquad (3.32)$$

$$P_{kj,iq} = \frac{f(\epsilon_>)/f(\epsilon_<) - 1}{\epsilon_j - \epsilon_k}M\langle j \mid V_{iq} \mid k \rangle \ ,$$

$$\tilde{P}_{kj,iq} = P_{kj,qi} \ ,$$

and $\epsilon_>$ denotes the greater of ϵ_j and ϵ_k and $\epsilon_<$ denotes the lesser.

Excluding degeneracies for simplicity, the eigenvalues of the stability matrix can be classified into two groups. The first class is the eigenvalues of the filter itself, which correspond to the case in which there is no self-consistency, $P = \tilde{P} = S = T = 0$. These eigenvalues are of the form $f(\epsilon_>)/f(\epsilon_<)$. The second class is the eigenvalues of the matrix

$$\mathscr{S} = \begin{bmatrix} S & T \\ T^* & S^* \end{bmatrix} \ , \qquad (3.33)$$

which carries information about self-consistency.

The necessary and sufficient condition for the particle-hole components $C_{kp}^{(n)}$ of the set $\{\phi_k^{(n)}\}$ to approach zero with iteration is that all eigenvalues of $\mathscr{S}$ have an absolute value less than 1. The hole-hole components will approach zero if the filter is convergent for the linear problem.

C. Energy-stability and filter convergence

To understand the convergence of the filter method, it is instructive to express the particle-hole component of the filter stability matrix $\mathscr{S}$ in terms of the Thouless energy stability matrix.

For our energy functional,

$$\mathscr{E}[\phi] = -M\sum_{k=1}^{A}\int d\mathbf{x}\,\phi_k^*\nabla_x^2\phi_k$$

$$+ \tfrac{1}{2}\int d\mathbf{x}\,d\mathbf{y}\,\rho(\mathbf{x})v(\mathbf{x}-\mathbf{y})\rho(\mathbf{y}) + \tfrac{1}{3}V_\delta\int d\mathbf{x}\,\rho^3(\mathbf{x}) \ ,$$

$$(3.34)$$

denoting the particle-hole amplitudes of the $\phi_k^{(n)}$ in the basis of Hartree eigenstates ϕk as $c_{kp}^{(n)}$ as before, the energy as a function of the C's may be written[7]

$$E^{(n)} - E = \tfrac{1}{2}(C^*C)\begin{bmatrix} A & B \\ B^* & A^* \end{bmatrix}\begin{bmatrix} C \\ C^* \end{bmatrix} \ , \qquad (3.35)$$

where

$$A_{kp,jq} = (\epsilon_p - \epsilon_k)\delta_{kj}\delta_{pq} + M\langle p \mid V_{jq} \mid k \rangle ,$$

$$B_{kp,jq} = M\langle p \mid V_{qj} \mid k \rangle . \tag{3.36}$$

Note from the definition of V_{iq}, Eq. (3.26), that $\langle p \mid V_{iq} \mid k \rangle^* = \langle k \mid V_{qi} \mid p \rangle$ and $\langle p \mid V_{iq} \mid k \rangle = \langle q \mid V_{pk} \mid i \rangle$, so that A is Hermitian and B is symmetric. Hence, the energy stability matrix is Hermitian and has real eigenvalues which we denote as follows

$$\mathcal{T} \mid \xi^{(\nu)} \rangle = \sigma^{(\nu)} \mid \xi^{(\nu)} \rangle ,$$

$$\mathcal{T} \equiv \begin{bmatrix} A & B \\ B^* & A^* \end{bmatrix} , \tag{3.37}$$

$$\mid \xi^{(\nu)} \rangle = \begin{bmatrix} u^{(\nu)} \\ v^{(\nu)} \end{bmatrix} .$$

For the functional $\mathcal{E}[\phi]$ to have a stable minimum, all these eigenvalues must be positive. In this section we will use the physical fact that $\mathcal{T}$ has positive eigenvalues to establish conditions on the eigenvalues of the particle-hole filter stability matrix.

Let us rewrite the matrices S and T in Eq. (3.32), making up $\mathcal{S}$ as follows:

$$S_{kp,jq} = \delta_{pq}\delta_{kj} - \frac{1 - f(\epsilon_p)/f(\epsilon_k)}{\epsilon_p - \epsilon_k}$$

$$\times [(\epsilon_p - \epsilon_k)\delta_{pq}\delta_{kj} + M\langle p \mid V_{iq} \mid k \rangle] ,$$

$$\tag{3.38}$$

$$T_{kp,jq} = -\frac{1 - f(\epsilon_p)/f(\epsilon_k)}{\epsilon_p - \epsilon_k} M\langle p \mid V_{qi} \mid k \rangle ,$$

and define the matrix

$$J_{kp,jq} = \delta_{kj}\delta_{pq} \frac{1 - f(\epsilon_p)/f(\epsilon_k)}{\epsilon_p - \epsilon_k} . \tag{3.39}$$

The filter stability matrix may then be written in terms of J and the energy stability matrix in the following form:

$$\mathcal{S} = 1 - J \begin{bmatrix} A & B \\ B^* & A^* \end{bmatrix}$$

$$= 1 - J\mathcal{T} . \tag{3.40}$$

Two particular choices of the filter function f yield especially simple iteration algorithms in common use. These correspond to the exponential filter $f(\hat{h}) = e^{\beta \hat{h}}$ in the limits of small β and large β, respectively. For small β, we obtain the linear filter

$$f_L(\hat{h}) = 1 - \beta \hat{h} , \tag{3.41}$$

in which case

$$\frac{1 - f_L(\epsilon_p)/f_L(\epsilon_k)}{\epsilon_p - \epsilon_k} \to \beta$$

and

$$\mathcal{S}_L = 1 - \beta \begin{bmatrix} A & B \\ B^* & A^* \end{bmatrix}$$

$$= 1 - \beta\mathcal{T} . \tag{3.42}$$

Since all the eigenvalues $\mathcal{T}$ are positive, it follows that all the eigenvalues of $\mathcal{S}$ are less than one. Let σ_m denote the largest eigenvalue of $\mathcal{T}$. As long as $\beta < 2/\sigma_m$, the most negative eigenvalue of $\mathcal{S}_L$ is greater than -1, so that all the particle-hole components of the wave functions are damped with iteration. Finally, choosing $\beta < 2/\epsilon_{max}$, where ϵ_{max} is the largest eigenvalue of $\hat{h}$ on the spatial lattice, also ensures that the filter converges for the linear problem. Hence, we may always find a β sufficiently small that the wave functions obtained by applying the linear filter (1.54) to an initial set of wave functions close to the Hartree eigenfunction will converge to the Hartree solution.

In the limit in which $\beta \to \infty$, the exponential filter

$$f_{exp}(\hat{h}^{(n)}) = e^{-\beta(\hat{h}^{(n)})} \tag{3.43}$$

diagonalizes the single-particle Hamiltonian $\hat{h}^{(n)}$. This yields the familiar Hartree iteration procedure in which the $(n + 1)$st iteration $\{\phi_k^{(n+1)}\}$ is composed of the eigenfunctions calculated in the potential generated by the nth iteration $\{\phi_k^{(n)}\}$. The same result is obtained if one uses a Legendre polynomial filter of sufficiently high degree that $\hat{h}^{(n)}$ is essentially diagonalized. For the Hartree method, Eq. (3.39) becomes

$$J_{kp,jq} \to \delta_{kj}\delta_{pq} \frac{1}{\epsilon_p - \epsilon_k} \equiv \left[\frac{1}{\Delta\epsilon} \right]_{kp,jq} , \tag{3.44}$$

and $\mathcal{S}$ may be written

$$\mathcal{S} = 1 - \left[\frac{1}{\Delta\epsilon} \right] \begin{bmatrix} A & B \\ B^* & A^* \end{bmatrix} \tag{3.45}$$

or, alternatively,

$$S_{kp,iq} = -\frac{1}{\epsilon_p - \epsilon_k} M\langle p \mid V_{iq} \mid k \rangle ,$$

$$T_{kp,iq} = -\frac{1}{\epsilon_p - \epsilon_k} M\langle p \mid V_{qi} \mid k \rangle . \tag{3.46}$$

We will see below that the eigenvalues of $\mathcal{S}$ for any filter yielding a positive definite $\mathcal{T}$ are less than 1.

The result (3.46) for the stability of Hartree iteration was first obtained by Levit[8] using perturbation theory. Indeed, applying first-order perturbation theory to the Schrödinger equation,

$$(\hat{h} + \delta V^{(n)})\phi_k^{(n+1)} = \epsilon_k^{(n+1)}\phi_k^{(n+1)} , \tag{3.47}$$

yields

$$C_{kp}^{(n+1)} = -\frac{\langle p \mid \delta V^{(n)} \mid k \rangle}{\epsilon_p - \epsilon_k} = S_{kp,jq}C_{jq}^{(n)} + T_{kp,jq}C_{jq}^{(n)*} . \tag{3.48}$$

We now consider the eigenvalues of $\mathcal{S} = 1 - J\mathcal{T}$ for a

general filter function f. The only conditions we impose on f is that it be a real and damp particles relative to holes; that is,

$$|f(\epsilon_p)| < |f(\epsilon_k)|, \quad \forall p > A, \quad k \leq A . \tag{3.49}$$

This condition ensures that the diagonal matrix J, Eq. (3.39), is positive definite, so we may define $J^{1/2}$ and its inverse $(J^{-1})^{1/2}$ is nonsingular. The matrix $\sqrt{J}\,\mathcal{T}\sqrt{J}$ is Hermitian and has a complete set of eigenvectors with real eigenvalues

$$\sqrt{J}\,\mathcal{T}\sqrt{J}\,|\chi_n\rangle = \lambda_n |\chi_n\rangle . \tag{3.50}$$

The eigenvalues are positive since $\lambda_n = (\langle \chi_n | \sqrt{J})\mathcal{T}(\sqrt{J} | \chi_n\rangle) > 0$ by the positivity of the energy stability matrix $\mathcal{T}$. Multiplication of Eq. (3.50) by $\sqrt{J}$ yields the eigenvalue equation for $J\mathcal{T}$,

$$J\mathcal{T}(\sqrt{J} | \chi_n\rangle) = \lambda_n(\sqrt{J} | \chi_n\rangle) . \tag{3.51}$$

Any vector $|V\rangle$ may be expanded in the set $\{\sqrt{J} | \chi_n\rangle\}$ since, by completeness, $(\sqrt{J})^{-1} | V\rangle$ may be expanded in $\{|\chi_n\rangle\}$. Thus, the eigenvalues $1 - \lambda_n$ of $\mathcal{S} = 1 - J\mathcal{T}$ are all less than unity and the particle-hole components will be damped with each iteration as long as $\lambda_n < 2$.

The only potential problem for any filter satisfying (3.49) is the possibility that some eigenvalue λ_n of (3.50) may be larger than 2. In this case, the component $(\sqrt{J} | \chi_n\rangle)$ is multiplied by $1 - \lambda_n$ at each iteration and gives rise to an alternating divergent series. This divergent sawtooth noise is a combination of the physics of the problem, embodied by the eigenvalues σ_m of the energy stability matrix which measure the curvature of the multidimensional energy surface, and the choice of the filter function f. Hence, this instability may be eliminated by suitable choice of the filter function. For example, we have already seen in the case of the linear filter, where $J = \beta$, that $\lambda_n = \beta\sigma_n$ and sawtooth noise may always be avoided by choosing β sufficiently small. A second alternative for the removal of a sawtooth instability is to use two or more previous iterations to define $\{\phi^{(n+1)}\}$, as described in Appendix C.

D. Constraints

As discussed in Sec. II, when we consider the mean field evolution in the space of Slater determinants, the Hartree energy plays the role of the potential energy. Hence, it is important to know the global structure of this multidimensional surface. One useful technique to explore this surface is to introduce a constraint—that is, to minimize the energy subject to the condition that the expectation value of an operator $\hat{Q}$ have a specific value Q_0. This yields a one-dimensional projection of the full energy surface. In the case of fission, it is convenient to choose $\hat{Q}$ to be the quadrupole operator, and the constrained energy of deformation curve $E(Q)$ yields an appropriate characterization of the fission barrier. A particularly important point on the energy of deformation curve is the saddle point, where the energy is stationary and the self-consistent result is independent of the constraint. Although the constraint does not affect the stationary solution, it crucially affects the stability and convergence of the filter.

At the fission saddle point, there is one direction in which the energy decreases and the energy stability matrix has one negative eigenvalue. This negative eigenvalue implies that one eigenvalue of the filter stability matrix is greater than one, and the iteration will not converge to the saddle point. Rather, it slides down the barrier toward one of the stable minima. To define a new problem which is stable, we add to the Hamiltonian the constraint

$$\mathscr{C}[\rho] = \tfrac{1}{2}\eta \left| \int d\mathbf{x}\rho(\mathbf{x})\hat{Q}(\mathbf{x}) - Q_0 \right|^2 . \tag{3.52}$$

This term adds a positive parabolic contribution centered at Q_0, so when the coefficient η is larger than the negative curvature at the saddle point, $\mathscr{C}[\rho] + \mathscr{C}[\rho]$ has a stable minimum. Note that the constraint $\mathscr{C}$ is equivalent to the Hartree energy functional obtained by adding to the Hamiltonian the one-body potential $\eta Q_0\hat{Q}(\mathbf{x})$ and the two-body separable interaction $v(\mathbf{x},\mathbf{y}) = \eta\hat{Q}(\mathbf{x})\hat{Q}(\mathbf{y})$. Thus, its contribution to the energy stability matrix is obvious: The one-body potential affects the location of the minimum, but does not contribute to the quadratic form (3.35). By Eq. (3.36), the contribution of the separable two body interaction yields

$$\mathcal{T}_c = \mathcal{T} + \eta \begin{bmatrix} \langle p | \hat{Q} | k \rangle\langle j | \hat{Q} | q \rangle & \langle p | \hat{Q} | k \rangle\langle q | \hat{Q} | j \rangle \\ \langle p | \hat{Q} | k \rangle^*\langle q | \hat{Q} | j \rangle^* & \langle p | \hat{Q} | k \rangle^*\langle j | \hat{Q} | q \rangle^* \end{bmatrix} . \tag{3.53}$$

With a choice of η and $\hat{Q}$ such that $\mathcal{T}_c$ is positive, it follows by our previous argument that the eigenvalues of the filter stability matrix are less than 1. As long as η is not so large that eigenvalues are pushed below -1, the iterative filter will converge as the desired solution.

Having introduced constraints, an obvious question is how to optimize them. Eq. (3.53) provides significant guidance. Suppose we wish to control one particular mode of the stability matrix, say, for example, an unstable mode or the one which has eigenvalue closest to one and hence is the most slowly converging. In the notation of Eq. (3.37) let

$$| \xi^{(v)}\rangle = \begin{bmatrix} u^{(v)} \\ v^{(v)} \end{bmatrix}$$

denote the mode of interest and define the constraint Q such that its particle-hole matrix elements are proportional to this mode:

$$\langle p | \hat{Q} | k \rangle = u_{kp}^{(v)} , \tag{3.54}$$

$$\langle k | \hat{Q} | p \rangle = v_{kp}^{(v)} .$$

The, by the orthonormality of the eigenvectors $| \xi^{(v)}\rangle$,

$$\mathcal{T}_c \mid \xi^{(\nu')} \rangle = (\sigma^{(\nu)} + \eta \delta_{\nu\nu'}) \mid \xi^{\nu'} \rangle , \tag{3.55}$$

where

$$(\mathcal{T}_c)_{kp,jq} = \mathcal{T}_{kp,jq} + \eta \xi_{kp}^{(\nu)} \xi_{jq}^{(\nu)*} . \tag{3.56}$$

Thus, the optimal constraint is given by the eigenfunction of the stability matrix. We will subsequently present graphs of relevant eigenmodes in illustrative cases. Even if one does not have a quantitative knowledge of the mode, a qualitative understanding can be extremely useful in approximately satisfying (3.54) and thus controlling the structure of the stability matrix and improving the convergence rate.

IV. THE TIME-DEPENDENT HARTREE PROBLEM

Having shown the essence of the filter method for the static problem, we now address the new features which arise in the time-dependent Hartree problem. As discussed in Sec. II, there are two alternative self-consistent eigenvalue problems which specify the bounce solution, Eqs. (2.19) and (2.14), and we will consider each in turn.

A. Naive time discretization and spurious states

The most straightforward generalization of the method applied to the Hartree problem in the preceding section is to solve Eq. (2.19) iteratively by applying a filter $f[\partial/\partial\tau + \hat{h}_\sigma(\mathbf{x},\tau)]$ to a set of time-dependent wave functions $\{\phi_k^{(N)}(\mathbf{x},\tau)\}$. Because all eigenvalues for family members in the time continuum have the same real part, Eq. (2.23), and differ only by a phase factor (2.22), Graham-Schmidt orthogonalization at each time slice according to the scalar product

$$\int d\mathbf{x}\, \phi_k(\mathbf{x}, -\tau)\phi_k(\mathbf{x},\tau) \tag{4.1}$$

has the property of selecting one function from each of the A lowest families.

We now replace the differential operators in (2.19) by discrete difference operators on a space-time lattice and write

$$(D_\tau + \hat{h}_\sigma)_{ij}\phi_{an}(\mathbf{x}_i,\tau_j) = \lambda_{an}\phi_{an}(\mathbf{x}_i,\tau_j) . \tag{4.2}$$

The fundamental difference between this problem and the continuum problem is the fact that Eq. (2.22) no longer holds. Thus, family members are no longer multiplies of a phase factor times a single fundamental solution, and Graham-Schmidt orthogonalization using Eq. (4.1) will allow population of more than one state of the lowest family at the expense of not populating higher families.

For a difference operator of the antisymmetric form

$$D_\tau \phi(n) = \frac{\phi(n+1) - \phi(n-1)}{2\Delta\tau} ,$$

or

$$D_\tau \phi(n) = \frac{-\phi(n+2) + 8\phi(n+1) - 8\phi(n-1) + \phi(n-2)}{12\Delta\tau} , \tag{4.3}$$

the spectrum has approximately the same form as Eq.

(2.23), with N_τ family members having approximately equal real parts. The modes with the largest imaginary parts correspond to time sawtooth modes, with the sign changing at each time slice. Clearly, these modes are dominated by artificial finite mesh effects, and since the time and spatial structure are strongly coupled, the spatial behavior of these modes is also unphysical. Thus, to the extend to which these modes are not orthogonal to the fundamental family members, the nonorthogonal component is completely unphysical. If the Graham-Schmidt orthogonalization allows these components to replace higher fundamental family members, the algorithm is replacing physics by noise.

One way to remove such time sawtooth modes from the problem is to use a nonantisymmetric difference operator such as

$$D_\tau \phi(n) = \frac{\phi(n) - \phi(n-1)}{\Delta\tau}$$

or

$$D_\tau \phi(n) = \frac{\phi(n-2) - 6\phi(n-1) + 3\phi(n) + 2\phi(n+1)}{6\Delta\tau} , \tag{4.4}$$

which gives rise to an eigenvalue spectrum of the form shown in Fig. 2. In this case, the mode in each family with the largest τ variation, and thus the greatest discretization noise, have the largest real part in their eigenvalues and are thus preferentially removed by the filter.
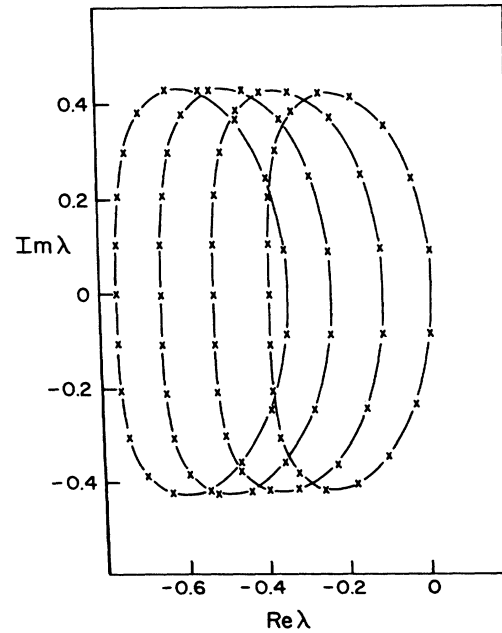
FIG. 2. Eigenvalue spectrum λ_{na} of the periodic time dependent Hartree eigenvalue problem, Eq. (4.2), with a nonantisymmetric discrete difference operator, Eq. (4.4). This spectrum was calculated for the model described in Sec. VI for 16 particles using 19 time slices. The solid lines connect eigenvalues corresponding to a single family.

The practical issue in implementing this method is to arrange for the noisy members of each family to be pushed up above the energy of the highest occupied fundamental state. Since the separation between the physical modes and those dominated by lattice noise varies as $1/\Delta\tau$, we must have $1/\Delta\tau$ greater than the difference between the largest and smallest single-particle energies of occupied states, typically $1/\Delta\tau > 40$ MeV. For heavy nuclei, known mass parameters and fission barrier curvatures[9] imply that the oscillator frequency of the inverted well at the fission barrier is of the order of $\omega \approx 300$ keV. Since the bounce period T must be larger than the period for small amplitude oscillations around the saddle point, $T > 2\pi/\omega$, the number of time slices required to implement this method is

$$N_\tau = \frac{T}{\Delta\tau} > \frac{2\pi}{0.3 \text{ MeV}} \times 30 \text{ MeV} \sim 840 . \qquad (4.5)$$

Considering the fact that each spatial dimension must have of the order of 20 mesh points, requiring 10^3 time slices, a total lattice size of $(20)^3 \times 10^3$ is computationally prohibitive. Thus, although the solution of Eq. (4.2) by the same filter method as applied to the static Hartree problem is suitable for very light nuclei such as the ^{8}Be example of Ref. 1, it is not practical for heavy nuclei.

B. Exact time evolution in a piecewise continuous potential

Because of the spurious family members associated with naive discretization of Eq. (2.19), the method of choice is to solve the Hermitian eigenvalue problem (2.14) in three spatial dimensions. Since the wave functions are only defined on discrete time slices, the density $\sigma(\mathbf{x},\tau)$ defining the potential in the time continuum is given by Eqs. (2.27) and (2.28). That is, the potential in the interval $\tau_i < \tau < \tau_{i+1}$ is a constant equal to the potential generated by the average of the density at τ_i and τ_{i+1}. Because we effectively solve continuum equations in a potential defined in the time continuum, there are no difficulties associated with spurious family members.

Equation (2.14) yields the single-particle wave functions at the time slice corresponding to $-T/2$. From there, the wave functions at subsequent time slices are obtained using the evolution operator $U(\tau_{i+1},\tau_i) = e^{-\Delta\tau h[\sigma(\tau_i+1/2)]}$, Eq. (2.26), where the exponential is evaluated either as a Taylor series or using the Napier formula. Since the bounce solution approaches the ground state Hartree solution as $T \to \infty$, the eigenfunctions $\psi_\alpha(\mathbf{x}, -T/2)$ will approach ground state wave functions and the eigenvalue will approach $\Lambda_\alpha = e^{-\epsilon_\alpha T}$, where ϵ_α is the Hartree single-particle energy. The occupied single-particle states correspond to the A largest eigenvalues Λ.

We solve the eigenvalue problem

$$U_\sigma \psi_\alpha(\mathbf{x}, -T/2) = \Lambda_\alpha \psi_\alpha(\mathbf{x}, -T/2)$$

using the filter method. Because the eigenvalues $\Lambda_\alpha = e^{-\epsilon_\alpha T}$ decrease exponentially, the simple filter $f(U) = U^N$, where N is a small integer, is adequate. The iteration scheme is defined as follows.

1. Initialization

A set of single particle wave functions $\{\phi_\alpha^{(0)}(\mathbf{x})\}$ is selected to approximate $\{\psi_\alpha(\mathbf{x}, -T/2)\}$ and a time-even potential $\sigma^{(0)}(\tau_{i+1/2}) = \sigma^{(0)}(-\tau_{i+1/2})$ is chosen. In practice, it is efficient to define ϕ_α^0 and $\sigma^{(0)}(\tau_{i+1/2})$ from appropriate constrained Hartree solutions.

2. Iteration

a. Application of filter. Let $\phi_\alpha^{M,0}$ denote the approximation to $\psi_\alpha(\mathbf{x}, -T/2)$ at the Mth iteration and $\phi_\alpha^{M,k}$ denotes the result of applying the evolution operator to $\phi_\alpha^{M,0}$ k times. The $(k+1)$st application of the evolution operator proceeds as follows. The wave function with the highest eigenvalue, $\phi_1^{(M,k)}(\mathbf{x}_j)$, is evolved from the first time slice τ_1 to the last time slice τ_L using the evolution operator

$$U(\tau_{i+1},\tau_i) = e^{-\Delta\tau h[\sigma^M(t_{i+1/2})]} .$$

The resulting wave function is denoted $\mathcal{X}_1(\mathbf{x}_j, \tau_i)$ and normalized according to

$$\sum_j \Delta x \mathcal{X}_1(\mathbf{x}_j, -\tau_i) \mathcal{X}_1(\mathbf{x}_j, \tau_i) = 1 .$$

The wave function with the second largest eigenvalue, $\phi_2^{(M,k)}(\mathbf{x}_j)$, is evolved with $U(\tau_{i+1},\tau_i)$, orthogonalized to $\mathcal{X}_1$ by imposing

$$\sum_j \Delta x \mathcal{X}_1(\mathbf{x}_j, -\tau_i) \mathcal{X}_2(\mathbf{x}_j, \tau_i) = 0 ,$$

and normalized. Each remaining wave function is evolved in order of decreasing eigenvalue, orthogonalized to all preceding wave functions, and normalized. Finally, the set of wave functions at the last time slice, $\{\mathcal{X}_\alpha(\mathbf{x}_i, \tau_L)\}$ is orthogonalized, the resulting orthonormal wave functions are denoted $\{\phi_\alpha^{M,k+1}\}$, and the process of applying the evolution operator is repeated. When the evolution operator has been applied N times, the resulting wave functions are denoted $\psi_\alpha^{(M+1)}(\mathbf{x}_j, \tau_i)$ and $\phi_\alpha^{M+1,0} = \psi_\alpha^{(M+1)}(\mathbf{x}_j, \tau_i)$.

b. Evaluation of $\sigma^{(M+1)}(\mathbf{x},\tau)$. The approximate eigenfunctions $\{\psi_\alpha^{(M+1)}\}$ of $U_{\sigma^{(M)}}$ are used to calculate

$$\sigma^{(M+1)}(\mathbf{x}_j, \tau_i) = \sum_\alpha \psi_\alpha^{(M+1)}(\mathbf{x}_j, -\tau_i) \psi_\alpha^{(M+1)}(\mathbf{x}_j, \tau_i) ,$$

from which $U_{\sigma^{(M)}}(\tau_{i+1}, \tau_i)$ is calculated from Eqs. (2.26) and (2.27) Steps a and b of the iteration process are then repeated using the initial wave functions $\phi_\alpha^{(M+1),0}$ and evolution operator $U_{\sigma^{(M+1)}}$.

The only new feature in the iteration algorithm which requires comment is the orthogonalization of the single particle wave functions. Suppose we expand the approximate eigenfunctions of U, $\{\phi_\alpha\}$, in the exact eigenfunctions $\{\psi_\alpha\}$,

$$\phi_\alpha = \sum_k C_{\alpha k} \psi_k . \qquad (4.6)$$

Then,

$$U\left[\frac{T}{2}, -\frac{T}{2}\right]\phi_\alpha = \sum_k C_{\alpha k}e^{-\epsilon_k T}\psi_k \ . \tag{4.7}$$

For the lowest state ϕ_1, there is no problem if there are small admixtures of other states, because these admixtures will be exponentially damped with a factor $e^{-(\epsilon_2-\epsilon_1)T}$ For the second state, however, even a very small contaminant C_{21} will get exponentially enhanced by the factor $e^{(\epsilon_2-\epsilon_1)T}$. The worst case will be the contaminant of ψ_1 in ϕ_A. Using our earlier estimate of $T > 2\pi/\omega$, with $\omega \sim 300$ keV and $\epsilon_A - \epsilon_1 \sim 40$ MeV, the exponential factor would be $e^{(\epsilon_A-\epsilon_1)T} \sim e^{840}$. Thus, noise associated with infinitesimal admixtures of lower eigenstates will totally dominate the results, unless these lower modes are explicitly removed by orthogonalization at each step.

C. Stability analysis

To the extent to which the filter $f(U_\sigma) = U_\sigma^N$ determines the exact eigenfunctions of U_σ, the iterative procedure presented in the preceding subsection corresponds to the Hartree method. To simplify the stability analysis, we will use perturbation theory for the Hartree method first in the space-time continuum and subsequently on the lattice.

Let $\{\phi_{\kappa k}^{(N)}\}$ denote the occupied states at iteration N obtained by diagonalizing

$$(\partial_\tau + \hat{h}^{(N-1)})\phi_{\kappa k}^{(N)} = \lambda_{\kappa k}^{(N)}\phi_{\kappa k}^{(N)} \ , \tag{4.8}$$

with normalization

$$\frac{1}{T}\int_{-T/2}^{T/2}d\tau\int d\mathbf{x}\,\phi_{\kappa'k'}(\mathbf{x}, -\tau)\phi_{\kappa,k}(\mathbf{x},\tau) = \delta_{\kappa'\kappa}\delta_{k'k} \ . \tag{4.9}$$

Greek indices denote spatial quantum numbers and the Roman indices indicate family members differing by time phase factors. Consistent with previous notation, $\{\kappa k, \lambda l\}$ denote occupied states, $\{\rho p, \sigma s\}$ denote unoccupied states, and $\{\alpha a, \beta b\}$ run over all states. The solutions at the Nth iteration are expanded as follows:

$$\phi_{\kappa k}^{(N)} = \phi_{\kappa k} + \sum_{\lambda l}C_{\kappa k\lambda l}^{(N)}\phi_{\lambda l} + \sum_{\rho p}C_{\kappa k\rho p}^{(N)}\phi_{\rho p} \ , \tag{4.10}$$

where the time phase factors Eq. (2.22) imply

$$C_{\kappa k\alpha a}^{(N)} = C_{\kappa 0\alpha(a-k)}^{(N)} \ , \tag{4.11}$$

and, to first order in the C's, orthogonality yields

$$C_{\kappa k\kappa'k'}^{(N)} + C_{\kappa'k'\kappa k}^{(N)} = 0 \ . \tag{4.12}$$

The density may be written

$$\rho^{(N)} = \sum_\kappa \phi_{\kappa 0}^{(N)}(-\tau)\phi_{\kappa 0}^{(N)}(\tau)$$

$$= \rho + \sum_{\lambda l}C_{\kappa 0\lambda l}^{(N)}[\phi_{\kappa 0}(-\tau)\phi_{\lambda l}(\tau) + \phi_{\kappa 0}(\tau)\phi_{\lambda l}(-\tau)]$$

$$+ \sum_{\rho p}C_{\kappa 0\rho p}^{(N)}[\phi_{\kappa 0}(-\tau)\phi_{\rho p}(\tau) + \phi_{\kappa 0}(\tau)\phi_{\rho p}(-\tau)] \ . \tag{4.13}$$

The hole-hole contributions vanish identically, as is seen by relabeling indices and using Eqs. (4.11) and (4.12) as follows:

$$\sum_{\kappa\lambda l}C_{\kappa 0\lambda l}[\phi_{\kappa 0}(-\tau)\phi_{\lambda l}(\tau) + \phi_{\kappa 0}(\tau)\phi_{\lambda l}(-\tau)]$$

$$= \sum_{\kappa\lambda l}C_{\kappa 0\lambda l}[\phi_{\kappa-l}(-\tau)\phi_{\lambda 0}(\tau) + \phi_{\kappa-l}(\tau)\phi_{\lambda 0}(-\tau)]$$

$$= \sum_{\kappa\lambda l}C_{\lambda 0\kappa-l}[\phi_{\lambda l}(-\tau)\phi_{\kappa 0}(\tau) + \phi_{\lambda l}(\tau)\phi_{\kappa 0}(-\tau)]$$

$$= -\sum_{\kappa\lambda l}C_{\kappa 0\lambda l}[\phi_{\lambda l}(-\tau)\phi_{\kappa 0}(\tau) + \phi_{\lambda l}(\tau)\phi_{\kappa 0}(-\tau)]$$

$$= 0 \ , \tag{4.14}$$

so that

$$\delta\rho^{(N)} = \sum_{\rho p}C_{\kappa 0\rho p}^{(N)}[\phi_{\kappa 0}(-\tau)\phi_{\rho p}(\tau) + \phi_{\kappa 0}(\tau)\phi_{\rho p}(-\tau)] \ . \tag{4.15}$$

Hence, using first-order perturbation theory

$$C_{\kappa 0\rho p}^{(N)} = \frac{(\phi_{\rho p}(-\tau)\,|\,\Delta V^{(N-1)}\,|\,\phi_{\kappa 0})}{\lambda_{\kappa 0} - \lambda_{\rho p}} \ , \tag{4.16}$$

so that

$$C_{\kappa 0\rho p}^{(N)} = \mathscr{S}_{\kappa 0\rho p, \kappa'0\rho'p'}C_{\kappa'0\rho'p'}^{(N)} \ , \tag{4.17}$$

where

$$\mathscr{S}_{\kappa 0\rho p, \kappa'0\rho'p'} = \frac{(\rho p\kappa'0\,|\,v\,|\,\kappa 0\rho'p') + (\rho p\rho'p'\,|\,v\,|\,\kappa 0\kappa'0)}{\lambda_{\kappa 0} - \lambda_{\rho p}} \tag{4.18}$$

and

$$(\alpha a\beta b\,|\,v\,|\,\alpha'a'\beta'b') = \frac{1}{T}\int_{-T/2}^{T/2}d\tau\int d\mathbf{x}\,d\mathbf{y}\,\phi_{\alpha a}(\mathbf{x}, -\tau)\phi_{\beta b}(\mathbf{y}, -\tau)v(\mathbf{x}-\mathbf{y})\phi_{\alpha'a'}(\mathbf{x},\tau)\phi_{\beta'b'}(\mathbf{y},\tau) \ . \tag{4.19}$$

Just as a constraint was required to make the filter method converge for the static Hartree solution at the saddle point, so we must also introduce a constraint to make the present method stable for the bounce solutions. Hence, we add to the action the term

$$\mathscr{S}_c = \frac{1}{2}\eta\left[\frac{1}{T}\int_{-T/2}^{T/2}d\tau f(\tau)\int d\mathbf{x}\,\hat{Q}(\mathbf{x})\rho(x,\tau) - Q_0\right]^2 \ , \tag{4.20}$$

where $f(\tau)$ is an even function of time normalized such that

$$\frac{1}{T}\int_{-T/2}^{T/2}d\tau f(\tau) = 1 \ , \tag{4.21}$$

and $\hat{Q}(\mathbf{x})$ is a one-body operator as before, such as the quadrupole operator. The choice of $f(\tau)$ will be discussed in the next section. The contribution of (4.20) to the single-particle Hamiltonian is

$$h_c = \eta \left[\frac{1}{T} \int_{-T/2}^{T/2} d\tau f(\tau) \int d\mathbf{x}\, \hat{Q}(\mathbf{x})\rho(\mathbf{x},\tau) - Q_0 \right] f(\tau)\hat{Q}(\mathbf{x}) \ , \tag{4.22}$$

and including this constraint, the full stability matrix is

$$\mathscr{S}_{\kappa 0 pp,\kappa'0 p'p'} = \frac{(pp\kappa'0\,|\,v\,|\,\kappa 0 p'p') + (pp p'p'\,|\,v\,|\,\kappa 0\kappa'0) + 2\eta(pp\,|\,fQ\,|\,\kappa 0)(p'p'\,|\,fQ\,|\,\kappa'0)}{\lambda_{\kappa 0} - \lambda_{pp}} \ . \tag{4.23}$$

Since the theory on the discrete time lattice corresponds to exact time evolution in the continuum with a piecewise continuous potential, the lattice theory has essentially the same structure. It is convenient to write the eigenvalue problem on a discrete time lattice in the following block matrix form:

$$\begin{bmatrix} 0 & & & & & U(\tau_{N_{\tau_1}},\tau) \\ U(\tau_2\tau_1) & 0 & & & & \\ & U(\tau_3\tau_2) & 0 & & & \\ & & U(\tau_4\tau_3) & \ddots & & \\ & & & & 0 & \\ & & & U(\tau_{N_\tau-1}t_{N_\tau-2}) & 0 \end{bmatrix} \begin{bmatrix} \phi_{\kappa k}(\tau_1) \\ \phi_{\kappa k}(\tau_2) \\ \vdots \\ \phi_{\kappa k}(\tau_{N_\tau}) \end{bmatrix} = e^{-\lambda_a \Delta\tau} \begin{bmatrix} \phi_{\kappa k}(\tau_1) \\ \phi_{\kappa k}(\tau_2) \\ \vdots \\ \phi_{\kappa K}(\tau_{N_\tau}) \end{bmatrix} \ , \tag{4.24}$$

where $\phi_{\kappa k}(\tau_i)$ denotes the spatial wave function at the ith time slice. Perturbation theory applied to Eq. (4.24) yields

$$C_{\kappa 0 pp}^{(N)} = \frac{(\phi_{pp}(-\tau)\,|\,\delta U^{(N-1)}\,|\,\phi_{\kappa 0}(\tau))}{e^{-\lambda_{\kappa 0}\Delta\tau} - e^{-\lambda_{pp}\Delta\tau}} \ , \tag{4.25}$$

where $\delta U^{(N-1)}$ is the block matrix obtained by varying the block matrix U in Eq. (4.24). The discretized form of $\mathscr{S}$ following from (4.25) was used instead of the continuous expression (4.18) in the explicit calculations presented in Sec. VI.

V. PERIODIC SOLUTIONS IN THE VICINITY OF THE SADDLE POINT

A typical energy of deformation curve showing the energy as a function of quadrupole moment through the fission barrier is shown in Fig. 3. Although the curve was calculated for the particular model discussed in the next section, it is representative of the projection of the multidimensional energy surface for a general system obtained by constraining the quadrupole moment. Although one ultimate objective is to calculate the bounce solution denoted by the dashed line, which evolves from the Hartree metastable state M through the fission barrier and back, we will first consider the periodic solution denoted by the dotted line in the vicinity of the saddle point S. This solution is of interest for two reasons: it may be analyzed to a large extent analytically and it serves as a starting point for a practical calculation of the bounce.

To understand the periodic solutions corresponding to infinitesimal fluctuations around the saddle point, it is useful to recall the real-time random phase approximation (RPA) solution. Let $\{u_k\}$ denote the static Hartree solution at S, and write the solution to the time-dependent Hartree equations,

$$-i\partial_t \phi_k + \hat{h}\phi_k = \lambda_k \phi_k \ , \tag{5.1}$$

in the standard form,

$$\phi_k = u_k + \sum_p \mathscr{C}_{kp}(t)u_p \ , \tag{5.2}$$

with

$$\mathscr{C}_{kp}(t) + X_{kp}e^{-i\omega t} + Y_{kp}^* e^{i\omega t} \ . \tag{5.3}$$

FIG. 3. Constrained energy of deformation curve. The energy plus quadrupole constraint, Eq. (3.52), were minimized for the 16 particle system described in Sec. VI, and the resulting energy E is plotted as a function of the quadrupole moment $\langle Q \rangle$. The Hartree minimum for the metastable state M and the saddle point S are indicated. The dotted line denotes a periodic trajectory in the vicinity of the saddle point and the dashed line indicates the bounce trajectory governing spontaneous fission.

The infinitesimal amplitudes X_{kp}, Y_{kp} satisfy the RPA eigenvalue problem

$$\begin{bmatrix} A & B \\ -B & -A \end{bmatrix} \begin{bmatrix} X \\ Y \end{bmatrix} = \omega \begin{bmatrix} X \\ Y \end{bmatrix} , \qquad (5.4)$$

where A and B are the matrices (3.36) for real wave functions. As a result of the minus signs in the RPA matrix (5.4), which are not present in the energy stability matrix (3.37), the RPA matrix has complex frequencies when the stability matrix has negative eigenvalues. In particular, the unconstrained RPA problem at the saddle point has one complex frequency and all other frequencies are real. In imaginary time, when it is replaced by τ, the eigenvalue ω in Eq. (5.4) is replaced by $i\omega$. Hence, the real modes of the RPA problem correspond to exponentially growing modes in imaginary time, and the only candidate for a

periodic solution is the single mode which was exponentially increasing in real time.

Now consider the iteration stability matrix (4.23) for solution of the periodic eigenvalue problem in the vicinity of the saddle point. The exact eigenfunctions are the static Hartree wave function at the saddle point with the usual phase factors,

$$\phi_{\alpha a}(\mathbf{x}, \tau) = e^{i(2\pi a/T)\tau} u_\alpha(\mathbf{x}) . \qquad (5.5)$$

We will constrain the average value of the quadrupole moment over the period T to be Q_S, the quadrupole moment at the saddle point. That is, we use the constraint (4.22) with $f(\tau)$ equal to 1. Physically, this constraint prevents the entire trajectory from sliding away from the saddle point with iteration. The choice of a constant $f(\tau)$ ensures that the constraint only contributes for the fundamental family member

$$(\rho p \mid Q \mid \kappa 0) = \frac{1}{T} \int_{-T/2}^{T/2} d\tau \int d\mathbf{x}\, u_\rho(\mathbf{x}) e^{-i(2\pi p\tau/T)} Q(\mathbf{x}) u_\kappa(\mathbf{x}) = \int d\mathbf{x}\, u_\rho(\mathbf{x}) Q(\mathbf{x}) u_\kappa(\mathbf{x}) \delta_{p0} \equiv \langle p \mid Q \mid \kappa \rangle \delta_{p0} . \qquad (5.6)$$

Similarly, substituting the eigenfunctions (5.5) in (4.19), the matrix elements contributing to the stability matrix become

$$(\rho p \kappa' 0 \mid v \mid \kappa 0 \rho' p') = \delta_{pp'} \int d\mathbf{x}\, d\mathbf{y}\, u_\rho(\mathbf{x}) u_{\kappa'}(\mathbf{y}) v(\mathbf{x} - \mathbf{y}) u_\kappa(\mathbf{x}) u_{\rho'}(\mathbf{y}) = \delta_{pp'} \langle \rho \kappa' \mid v \mid \kappa \rho' \rangle \qquad (5.7)$$

and

$$(\rho p \rho' p' \mid v \mid \kappa 0 \kappa' 0) = \delta_{p,-p'} \langle \rho \rho' \mid v \mid \kappa \kappa' \rangle . \qquad (5.8)$$

With these results, the stability matrix may be written in the following simple block form:

$$\mathcal{S} = - \begin{bmatrix} \ddots & & & & & \cdot\cdot \\ & \Delta_{-2}^{-1}B & 0 & 0 & 0 & \Delta_{-2}^{-1}B \\ & 0 & \Delta_{-1}^{-1}B & 0 & \Delta_{-1}^{-1}B & 0 \\ & 0 & 0 & 2\Delta_0^{-1}B_0 & 0 & 0 \\ & 0 & \Delta_1^{-1}B & 0 & \Delta_1^{-1}B & 0 \\ & \Delta_2^{-1}B & 0 & 0 & 0 & \Delta_2^{-1}B \\ \cdot\cdot & & & & & \ddots \end{bmatrix} , \quad C = \begin{bmatrix} \vdots \\ C_{-2} \\ C_{-1} \\ C_0 \\ C_1 \\ C_2 \\ \vdots \end{bmatrix} , \qquad (5.9)$$

where all the particle-hole components of a given family index, C_m, are grouped together in a block, the diagonal matrix Δ_m is defined by

$$(\Delta m)_{\rho\kappa,\rho\kappa} \equiv \lambda_{\rho m} - \lambda_{\kappa 0} = \lambda_{\rho 0} + i\omega m - \lambda_{\kappa 0} , \qquad (5.10)$$

where $\omega = 2\pi/T$, B is the matrix (3.36) for real wave functions,

$$B_{\rho\kappa,\rho'\kappa'} = \langle \rho\rho' \mid v \mid \kappa\kappa' \rangle = (\rho\kappa' \mid v \mid \kappa\rho') , \qquad (5.11)$$

and the constraint only contributes to the $m = 0$ block,

$$B_{0\rho\kappa,\rho'\kappa'} = B_{\rho\kappa\rho'\kappa'} + \zeta \langle \rho \mid Q \mid \kappa \rangle \langle \rho' \mid Q \mid \kappa' \rangle . \qquad (5.12)$$

The eigenvalue equation for the stability matrix $\mathcal{S}$ separates into the following decoupled equations for each family label m:

$$-2\Delta_0^{-1}B_0 C_0 = S_0 C_0 , \qquad (5.13)$$

$$- \begin{bmatrix} \Delta_{-m}^{-1}B & \Delta_{-m}^{-1}B \\ \Delta_m^{-1}B & \Delta_m^{-1}B \end{bmatrix} \begin{bmatrix} C_{-m} \\ C_m \end{bmatrix} = S_m \begin{bmatrix} C_{-m} \\ C_m \end{bmatrix} . \qquad (5.14)$$

Equation (5.13) for the fundamental family $m = 0$ is precisely the static constrained Hartree stability eigenvalue problem discussed in Sec. III, and the eigenvalue S_0 may be rendered less than 1 by applying a single constraint at the saddle point.

The structure of the solutions for $m \neq 0$ may be seen by adding and subtracting the two independent equations in (5.14) to obtain

$$\begin{bmatrix} -(\Delta_{-m}^{-1} + \Delta_m^{-1})B & 0 \\ -(\Delta_{-m}^{-1} + \Delta_m^{-1})B & 0 \end{bmatrix} \begin{bmatrix} C_{-m} + C_m \\ C_{-m} - C_m \end{bmatrix} = S_m \begin{bmatrix} C_{-m} + C_m \\ C_{-m} - C_m \end{bmatrix} . \qquad (5.15)$$

If the dimension of the particle-hole space in each sector m is N, then Eq. (5.15) has N zero eigenvalues. Physically, the associated eigenfunctions correspond to modes having $C_m^* \neq C_{-m}$ which are forbidden by the restriction to real wave functions. Since

$$(\Delta_{-m}^{-1} + \Delta_m^{-1})_{\rho\kappa,\rho'\kappa'} = \frac{2(\lambda_{\rho 0} - \lambda_{\kappa 0})}{(\lambda_{\rho 0} - \lambda_{\kappa 0})^2 + \omega^2 m^2} \delta_{\rho\rho'}\delta_{\kappa\kappa'} \qquad (5.16)$$

is positive definite, the eigenvalue problem for the remaining N eigenfunctions may be written in the manifestly real symmetric form

$$[-(\Delta_m^{-1}+\Delta_{-m}^{-1})^{1/2}B(\Delta_m^{-1}+\Delta_{-m}^{-1})^{1/2}]\left[\frac{C_{-m}+C_m}{(\Delta_m^{-1}+\Delta_{-m}^{-1})^{1/2}}\right]$$

$$=S_m\left[\frac{C_{-m}+C_m}{(\Delta_m^{-1}+\Delta_{-m}^{-1})^{1/2}}\right], \quad (5.17)$$

so that the remaining N eigenvalues S_m are real. The limiting behavior of S_m as a function of period T can be seen by substituting Eq. (5.16) in Eq. (5.15) to obtain

$$-\left[\frac{(\lambda_{p0}-\lambda_{\kappa0})^2}{(\lambda_{p0}-\lambda_{\kappa0})^2+\omega^2m^2}\right]\frac{2}{\lambda_{p0}-\lambda_{\kappa0}}B_{\rho\kappa,\rho'\kappa'}(C_{-m}+C_m)_{\rho'\kappa'}$$

$$=S_m(C_{-m}+C_m)_{\rho'\kappa'}. \quad (5.18)$$

For T large enough that $2\pi/T=\omega\ll\lambda_{p0}-\lambda_{\kappa0}$, the quantity in large square brackets approaches 1 and Eq. (5.18) approaches the static unconstrained stability eigenvalue problem and therefore has one unstable mode with $S>1$. For T small enough that $2\pi/T=\omega\gg\lambda_{p0}-\lambda_{\kappa0}$, Eq. (5.18) approaches the static stability matrix multiplied by $1/\omega^2m^2$ and therefore all eigenvalues will approach zero. The qualitative behavior of the mode in each family which becomes unstable at large T is sketched in Fig. 4.

Of particular interest is the point at which each mode becomes unstable. For the value $S_m=1$, we may multiply the first and second lines of Eq. (5.14) by Δ_{-m} and Δ_m, respectively, and use (5.10) to obtain

$$\begin{bmatrix}(B+\Delta_0) & B \\ B & -(B+\Delta_0)\end{bmatrix}\begin{bmatrix}C_{-m} \\ C_m\end{bmatrix}=i\omega m\begin{bmatrix}C_{-m} \\ C_m\end{bmatrix}. \quad (5.19)$$

This result is precisely of the form of the imaginary time RPA eigenvalue problem [see Eqs. (5.4) and (3.42)] so that the "unstable" mode is just the desired periodic solution.
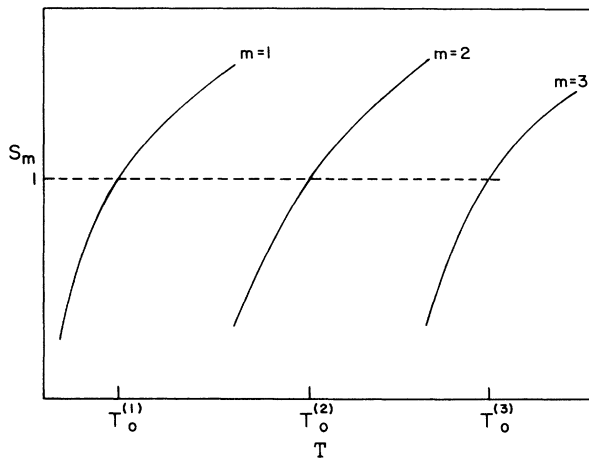
Note that if T_0 denotes the fundamental period corresponding to the desired RPA frequency $T_0=2\pi/\omega$, the period at which the mth family member becomes unstable is $T_0^{(m)}=mT_0$.

This stability analysis reveals an extremely convenient and practical way to find the RPA period and infinitesimal imaginary time periodic solutions. For a sequence of values of period T, we will define a set of initial time-dependent wave functions equal to the static Hartree saddle point wave functions modulated by an infinitesimal periodic dilational quadrupole scale transformation of period T. That is, the static solutions will be alternately infinitesimally stretched and compressed with period T and physically this shape deformation must have a substantial overlap with the true self-consistent periodic solution. The filter is then applied, and one observes whether the amplitude of the oscillation grows or damps with time. For a value of T smaller than the fundamental RPA period, the preceding analysis shows that all modes are stable so that the solution will converge to the static saddle point solution and the amplitude will decrease with iteration. As soon as T is increased slightly beyond the fundamental RPA period, the RPA mode will become unstable while all others remain stable. Hence, the amplitude of the RPA mode will grow with iteration. The onset of the stability thus defines the RPA period, and the growing component of the wave function gives the RPA eigenfunction. An explicit example will be shown in the next section.

For the study of fission, our primary interest in the RPA solution is as a starting point for calculating the large-amplitude bounce. Thus, once we have found the unstable mode, we simply iterate the solution for a series of increasing periods which yields solutions of larger and larger amplitude that eventually approach the bounce. The behavior of the energy of the resulting solution as a function of period is sketched in Fig. 5. For $T<T_0$, only static solutions exist, and the energy is the static energy at

FIG. 4. Sketch of the dependence of the stability eigenvalue for periodic solutions in the vicinity of the saddle point as a function of the period T. The single mode which becomes unstable in each family is denoted by the solid line. The period at which the eigenvalue $S_m=1$ is denoted $T_0^{(m)}$ and m is the family label.
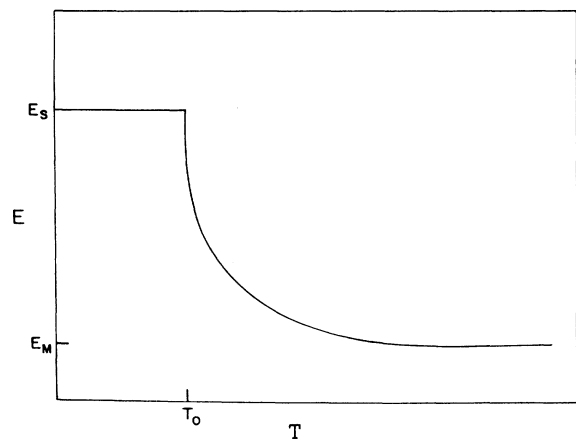

FIG. 5. Sketch of the energy of the periodic solution as a function of period T. As in Fig. 3, E_S denotes the energy of the saddle point and E_M denotes the static Hartree energy of the metastable parent state. The imaginary RPA time frequency is T_0.

the saddle point, E_S. At $T = T_0$, the energy is given by $E = E_S - A\omega_{RPA}$, where A is the RPA amplitude, so that $E(T)$ has infinite slope. As $T \to \infty$, the energy decreases monotonically, approaching the Hartree energy of the metastable state, E_M, from above. In practice, when T is several times larger than T_0, the solution is a good approximation to the bounce.

VI. RESULTS FOR AN ILLUSTRATIVE ONE-DIMENSIONAL MODEL

The salient results of the preceding section can be conveniently illustrated using the one-dimensional model of Ref. 1. The Hamiltonian density is of the Skyrme form

$$\mathcal{H}(\phi_\alpha(x,-\tau)\phi_\alpha(x,\tau)) = -M \sum_\alpha \phi_\alpha(x,-\tau)\frac{\partial^2}{\partial x^2}\phi_\alpha(x,\tau)$$

$$+ \tfrac{1}{2} \int dx' \rho(x,\tau)v(x-x')\rho(x',\tau)$$

$$+ \tfrac{1}{3} V_\delta \rho^3(x,\tau) , \tag{6.1}$$

where

$$V(x) = \sum_{j=1}^{2} \frac{V_j}{\sqrt{\pi}\gamma_j} e^{-x^2/\gamma_j^2} \tag{6.2}$$

and

$$\rho(x) = M \sum_\alpha \phi_\alpha(x,-\tau)\phi_\alpha(x,\tau) , \tag{6.3}$$

and lengths, energies, and times are measured in units of l_0, $E_0 = \hbar^2/2ml_0^2$, and $\tau_0 = \hbar/E_0$, respectively. The parameters used for a 16-particle system are the same as in Ref. 1 and those used to render an eight-particle system unstable with respect to breaking into two four-particle daughters are given in Table I. The kinetic energy is approximated by a five-point second difference operator using the mesh spacing Δx and number of lattice sites N_x given in the table. The analog of the quadrupole operator we have used in one dimension is $\hat{Q}(x) = x^2$.

A. Static properties

The constrained energy of deformation curve for symmetric fission has already been shown in Fig. 3. Here, we wish to consider the spatial density distribution shown in Fig. 6 associated with the lowest eigenmodes of the energy stability matrix at the saddle point.

The density distribution of the eight-particle system at the saddle point $\rho(x)$ is shown in Fig. 6(a). The simplest collective deformation one can apply to that density distribution to elongate it in the approximate direction of the

TABLE I. Parameters for the eight-particle model.

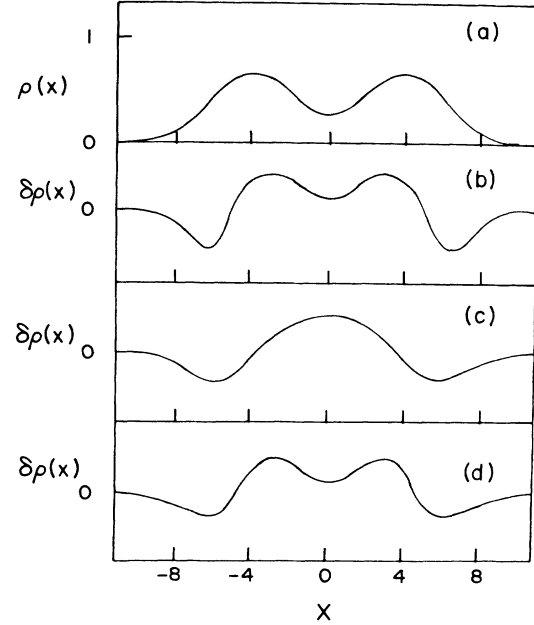|	
$\gamma_1 = 2$	$V_\delta = 0.5$
$\gamma_2 = 7$	$M = 4$
$V_1 = -1.489$	$N_x = 12$
$V_2 = 0.7$	$\Delta x = 1.975$

FIG. 6. Spatial density distribution for the eight particle model. The static Hartree distribution at the saddle point is shown in (a) and the pure dilation mode is shown in (b). The lowest (unstable) mode of the unconstrained energy stability matrix is shown in (c) and the analogous stable mode with a constraint of strength $\eta = 0.009$ is shown in (d).

fission path is the infinitesimal dilation

$$\rho_\epsilon(x) = (1+\epsilon)\rho((1+\epsilon)x) , \tag{6.4}$$

where the premultiplying factor is required for normalization. The resulting dilational density fluctuation

$$\delta\rho = \epsilon \frac{d}{d\epsilon}\rho\epsilon \bigg|_{\epsilon=0} = \epsilon(\rho + x\rho'(x)) , \tag{6.5}$$

as shown in Fig. 6(b).

The contribution to the density of a single mode of the energy stability matrix with particle-hole amplitudes C_{pk} for real wave functions is given by

$$\delta\rho = \sum_{p,k} C_{pk} u_p(x)u_k(x) . \tag{6.6}$$

In the absence of a constraint, the lowest mode is unstable and its contribution to the density is shown in Fig. 6(c). The addition of a constraint with $Q = x^2$ not only makes the eigenvalue positive, but also slightly alters the spatial distribution of the mode, as shown in Fig. 6(d). Aside from small details, however, the main conclusion from calculating the lowest eigenfunction of the stability matrix is that it has the qualitative behavior of the single dilational mode.

As discussed in Sec. III, the highest eigenmode of the stability matrix is the spatial sawtooth mode in which the sign of the wave function alternates between adjacent spatial mesh points. When the filter is chosen appropriately, the eigenvalue for this sawtooth mode is larger than -1 and virtually independent of the value of the constraint.
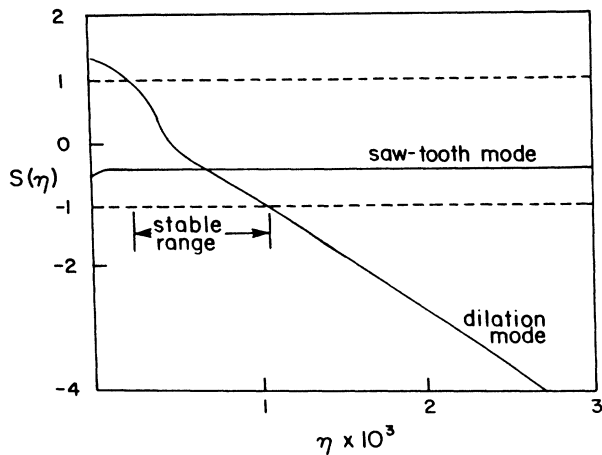
FIG. 7. Eigenvalues of the static filter stability matrix as a function of the constraint strength η for the sawtooth and dilation modes.

The overall structure of the stability eigenvalues as a function of the strength of the constraint η may be seen from Fig. 7. In the absence of a constraint, this dilation mode is the only mode greater than 1, and all other eigenvalues lie between 1 and the sawtooth eigenvalue. As η is increased, the dilation mode decreases monotonically. In the range for which it lies between 1 and -1, the filter method is stable and converges to the static saddle point solution. For η sufficiently large, the dilation eigenvalue falls below -1 and the filter becomes unstable.

B. Time-dependent solutions

The simplest time-dependent solution is the small-amplitude RPA oscillation around the saddle point discussed in detail in the preceding section. For the one-dimensional model, it is straightforward to diagonalize the real RPA matrix exactly, with the result that the RPA period is $T=41.3$ and the spatial distribution of $\delta\rho$ is identical to the curve plotted in Fig. 6(c).

One major question is the extent to which the structure of the finite-amplitude periodic solutions resembles the simple structure of the solutions we have analyzed in the vicinity of the saddle point. To study a representative finite-amplitude solution, we have calculated the periodic solution with $T=56$, which has an energy roughly midway between the saddle point and the Hartree minimum. The density distributions for this solution at the turning points $\rho(x,T/2)$ and $\rho(x,0)$ are shown in Fig. 8.

Two projections of the two highest eigenmodes of the time-dependent stability matrix are shown in Fig. 9. In the absence of a constraint, there is one unstable mode which we will refer to as the $D0$ mode. Its spatial distribution at fixed τ is shown in Fig. 9(a) and its time dependence at fixed x is shown in Fig. 9(c). At the saddle point, we know from the preceding section that the unstable mode of the unconstrained static stability matrix is an $m=0$ unstable eigenmode of the time-independent stability matrix. This mode has the spatial dependence shown by the dotted line in Fig. 9(a) and is a constant in time.
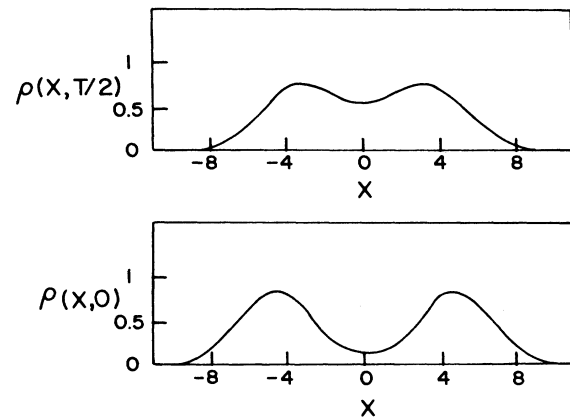

FIG. 8. Density profiles at $\tau=T/2$ and $\tau=0$ for a periodic solution with period $T=56$.

Thus, the $D0$ mode has the same qualitative behavior as the saddle-point dilational mode with $m=0$ (which motivates the notation $D0$) and we observe that at least in this case, the structure of the saddle point solutions is useful in characterizing finite amplitude solutions.

The second highest eigenmode shown in Figs. 9(b) and 9(c) is similarly related to the periodic RPA saddle point solution. Recall that at the RPA period, the $m=1$ family member with spatial dependence given by the RPA solution has stability eigenvalue 1. This solution factorizes
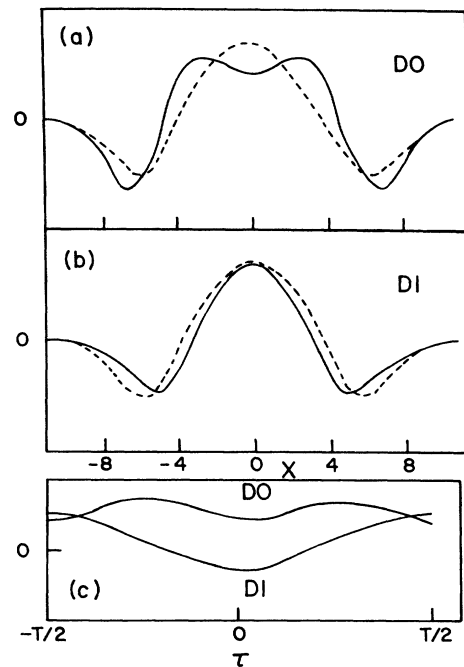

FIG. 9. Eigenmodes $D0$ and $D1$ of the stability matrix for the periodic solution with period $T=56$. The solid lines show $\delta\rho(x,\tau)$ for the $D0$ and $D1$ modes at fixed τ and at fixed x. For comparison, the dashed line in (a) and (b) shows the RPA solution at the saddle point, which to the accuracy of the figure, is identical with the unconstrained energy stability mode of Fig. 6(c).

into sinusoidal variations in time with period T and the RPA spatial dependence shown by the dashed line in Fig. 9(b), and thus has essentially the same structure as the $D1$ mode shown in Fig. 9. In this case the notation D again refers to the dilational spatial dependence and 1 denotes the $m = 1$ family member. For finite amplitude solutions, the $D1$ mode is stable and the $D0$ mode requires a constraint as in the static case. Because the time dependence of the $D0$ mode is approximately constant and the $D1$ mode is nearly sinusoidal, it is clear that a constraint of the form Eq. (4.22) with constant $f(\tau)$ will strongly couple to the $D0$ mode and nearly decouple from the $D1$ mode as in the saddle point analysis. In explicit calculations, we find that for $\eta = 0$, 4×10^{-3}, and 8×10^{-3}, the $D0$ eigenvalue is 1.22, 0.80, and -0.65, respectively, whereas in all three cases the $D1$ eigenmode is 0.92. Thus, for a constraint greater than 4×10^{-3} the convergence is satisfactory, with all eigenvalues being less than 0.92 and thus the slowest decaying contaminant being damped by 8% each iteration.

The qualitative effect of the $D0$ and $D1$ modes on the trajectory is sketched in Fig. 10. Assume we start with an exact periodic trajectory connecting inner turning point A and outer turning point B. Since the $D0$ mode is approximately constant in time, if the sign of the admixture is such that the quadrupole moment at the outer turning point B is increased to B', then the inner turning point A is also increased to A' and vice versa. The entire trajectory thus slides toward the Hartree minimum or toward the scission point just like the static solution slides away from the saddle point in the absence of a constraint. Again it is clear physically that a time-averaged constraint will control such a mode. Because of the sinusoidal time dependence of the $D1$ mode, the inner and outer turning points both move outward or inward as shown. If one wants to control the $D1$ mode with a constraint, one must pick a function $f(\tau)$ which has opposite signs at $\tau = 0$ and $T/2$. Just as the $D0$ eigenvalue may be pushed below 1 to improve convergence, so adding a second constraint to push

the second highest $D1$ eigenvalue further below 1 can also dramatically improve convergence, as will be seen in Fig. 14. A convenient alternative to using one constraint with $f(\tau)$ constant and a second constraint with $f(\tau)$ having a node between 0 and $T/2$ is to separately constraint $Q(T/2)$ and $Q(0)$.

C. Efficient calculation of the bounce

Finally, we now consider the main steps in a practical calculation of the bounce using the filter technique as it is to be applied to a large problem which could not be diagonalized by brute force.

The first problem is to find the RPA period and periodic small-amplitude solution. We begin with a constrained static saddle point density, and add to it a small periodic dilational component with spatial dependence $\delta\rho(x)$ given by Eq. (6.5) and sinusoidal time dependence. For each value of the period T, the Hartree iteration procedure of Sec. IV is applied to determine whether or not there is an unstable mode. The exact stability eigenvalue of the $m = 1$ unstable mode sketched in Fig. 4 was calculated explicitly for the present model, and the results are shown in Fig. 11. One observes that the mode has the expected behavior so the mode will grow whenever T exceeds the RPA T_0. Furthermore, except at the largest values of the period, replacing the time continuum by 16 time slices yields negligible error.

The behavior of the filter iterations for various values of T is summarized in Fig. 12, where the quadrupole moment at the outer turning point is plotted as a function of the iteration number. Note that, in general, the dilational starting *ansatz* will contain admixtures of other modes besides the RPA mode. Hence, even if the RPA amplitude
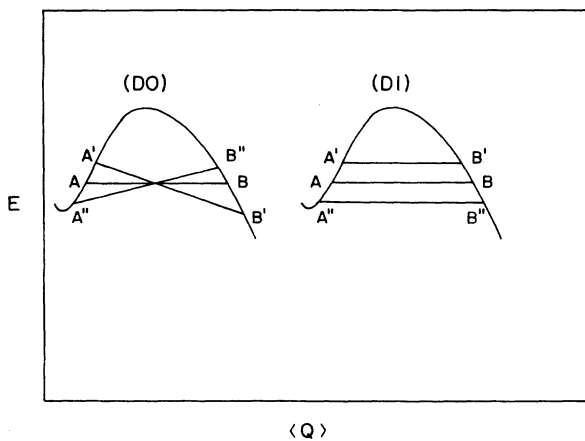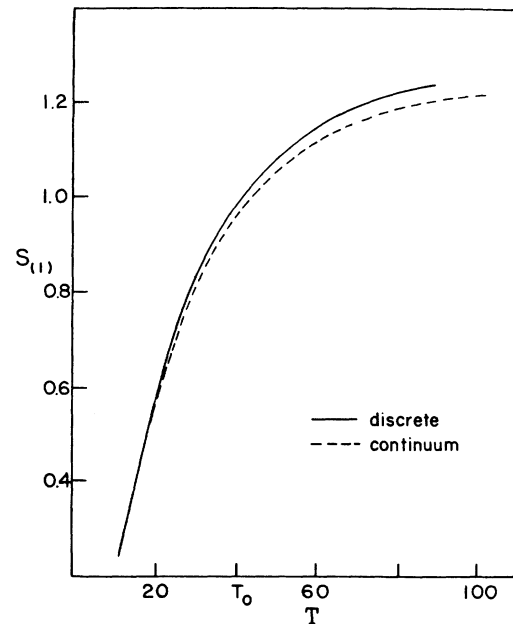

FIG. 10. Schematic representation of the $D0$ and $D1$ modes discussed in the text. The line AB represents the projection of the periodic trajectory in the $E - \langle Q \rangle$ plane. The lines $A'B'$ and $A''B''$ represent the result of adding and subtracting small components of $D0$ and $D1$ modes.

FIG. 11. Stability eigenvalue for the periodic solution in the vicinity of the saddle point as a function of period T. The RPA period is denoted by T_0.
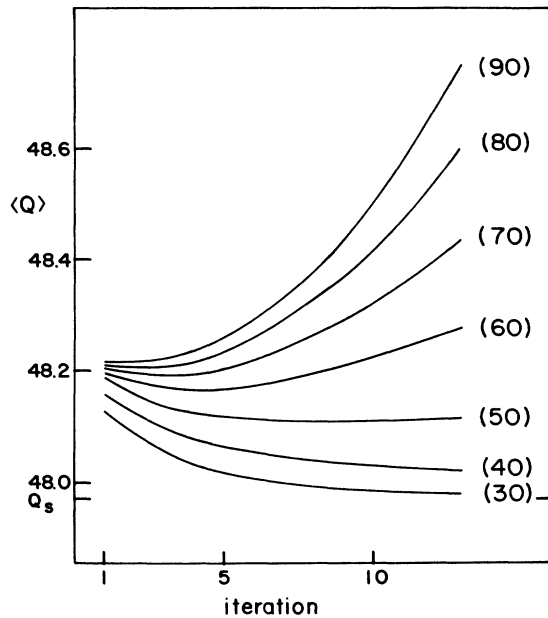
FIG. 12. Quadrupole moment $\langle Q \rangle$ at the outer turning point as a function of iteration. For a period (indicated in parentheses) less than the RPA period $T_0 = 49.5$, the initial small amplitude oscillation decays so that $\langle Q \rangle$ approaches the static saddle point value Q_S. For period greater than T_0, the amplitude eventually grows with iteration, displaying the instability discussed in Sec. V.

grows slowly with iteration, these other modes will decay and at first the total quadrupole moment will decrease with iteration. After these other components have damped out, however, the curve will eventually begin to increase. We observe this behavior clearly in Fig. 12, where $T_0 = 49.5$. The first curve with $T > T_0$ is for
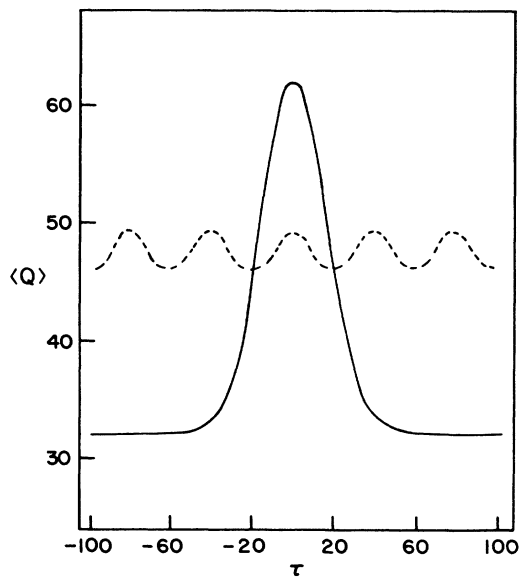
$T = 50$, and this curve decreases for the first seven iterations while stable modes are damped out, and only then slowly increases as the unstable eigenvalue slightly greater than 1 begins to dominate.

The second problem is to efficiently increase the period T and evolve the small amplitude oscillation into the bounce. Figure 13 shows the $\langle Q \rangle$ vs τ trajectory for the small amplitude RPA oscillation and the bounce solution. From this figure, it is quite plausible that one cycle of the RPA solution will smoothly deform into the bounce as T increases and this expectation is borne out in practice. One interesting and useful fact is that the width of the bounce is only about twice that of the RPA oscillation, so the RPA start indeed selects the appropriate time scale. As the period is increased beyond several times T_0, it is clear from this figure that the additional time is essentially all spent in the Hartree metastable state.

The most straightforward way to evolve from the RPA oscillation to the bounce solution is to maintain a single constraint on the average quadrupole moment and increase the period T. The resulting extremal values of Q at the inner and outer turning points are shown by the solid curves in Fig. 14. Although the method works, because the $D1$ eigenvalue is so close to 1, of the order of 80 iterations are needed for convergence which will pose a serious practical problem in large, computationally intensive applications. Hence, it is useful to introduce a second constraint as discussed previously to increase the rate at which the $D1$ mode is damped. The dashed lines in Fig. 14 show the convergence when $Q(T/2)$ and $Q(0)$ are separately constrained, and illustrate how the addition of a physically motivated constraint can increase the convergence rate by an order of magnitude.

FIG. 13. Quadrupole moment as a function of τ for small amplitude RPA oscillations around the saddle point (dashed curve) and for the bounce (solid curve).
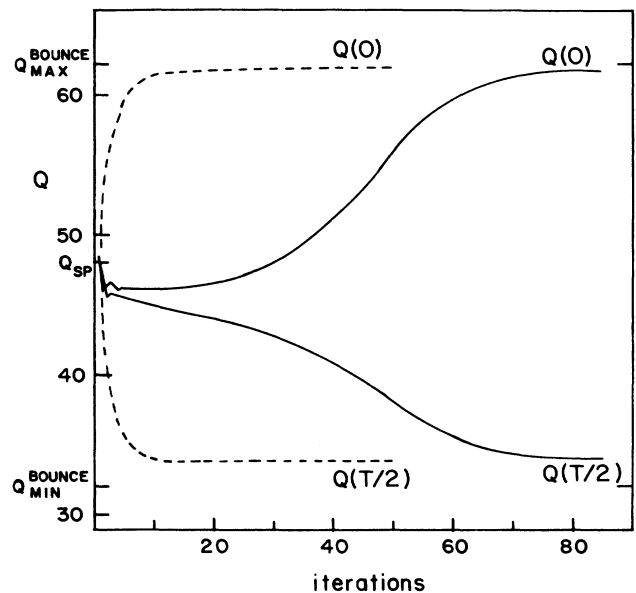

FIG. 14. Quadrupole moments of the inner and outer turning points as a function of iteration, starting from small oscillations around the saddle point. The solid line shows the result of a single constraint and the dashed line shows the enhanced convergence resulting from two constraints.

VII. SUMMARY AND CONCLUSIONS

In summary, we have presented a new iterative method for solving the fission bounce equations which is practical for large-scale calculations in three space-time dimensions with large numbers of occupied states. Instead of explicitly solving a large eigenvalue problem on a coordinate space mesh, the filter method only requires repeated multiplication of single-particle wave functions by a large sparse spatial difference matrix. Detailed stability analysis of alternative algorithms elucidated the pitfalls of naive time discretization and showed the need to effectively solve time continuum equations in a piecewise continuous potential to treat the family redundancy problem satisfactorily. The stability analysis also provided insight into the physical nature of the most slowly convergent and unstable modes and indicated how constraints could be introduced and optimized to control these modes.

The general theoretical ideas and practicality of the method were illustrated with a simple one-dimensional model which had been solved previously[1] by brute force. The computational strategy of finding the RPA period and small-amplitude periodic solution, and of increasing the period and introducing constraints to evolve this solution into the bounce was carried out in a way which generalizes directly to realistic three-dimensional calculations. Application of this method to three dimensional systems is presently in progress.

ACKNOWLEDGMENTS

APPENDIX A

In this appendix we derive Eq. (3.6). Since $\langle \phi_k^{(n)} | \phi_h^{(n)} \rangle = \delta_{kh}$ for $k, h = 1, 2, \ldots, A$, the matrix $\{ C_{kh}^{(n)} \}_{k,h=1,2,\ldots,A}$ is orthogonal. Hence, since the C's are small quantities, to order C^2 we may write

$$C_{kk} = 1 + \mathcal{O}(C^2) ,$$

$$C_{kh} + C_{hk} = 0 + \mathcal{O}(c^2) .$$

The Graham-Schmidt orthonormalization is applied in order of increasing eigenvalue. For the lowest eigenfunction

$$\phi_1^{(n)} = \phi_1 + \sum_{a \geq 2}^{\infty} C_{1a}^{(n)} \phi_a ,$$

application of the filter $f(\hat{h})$ gives

$$\bar{\phi}_1^{(n+1)} = f(\epsilon_1)\phi_1 + \sum_{a \geq 2}^{\infty} C_{1a}^{(n)} f(\epsilon_a)\phi_a ,$$

and normalization to leading order in C yields

$$\phi_1^{(n+1)} = \phi_1 + \sum_{a \geq 2}^{\infty} C_{1a}^{(n)} \frac{f(\epsilon_a)}{f(\epsilon_1)} \phi_a .$$

Hence, if

$$| f(\epsilon_a)/f(\epsilon_1) | < 1, \quad a = 2, \infty$$

then $| C_{1a}^{(n+1)} | < | C_{1a}^{(n)} |$ and $\phi_1^{(n)}$ will converge to the lowest state ϕ_1. Application of the filter to the other states yields

$$\bar{\phi}_k^{(n+1)} = f(\epsilon_k)\phi_k + \sum_{j \neq k}^{A} C_{kj}^{(n)} f(\epsilon_j)\phi_j + \sum_{p=A+1}^{\infty} C_{kp}^{(n)} f(\epsilon_p)\phi_p ,$$

and Graham-Schmidit orthogonalization yields

$$\phi_k^{(n+1)} = \phi_k + \sum_{j=1}^{k-1} C_{kj}^{(n)} \frac{f(\epsilon_k)}{f(\epsilon_j)} \phi_j + \sum_{p=k+1}^{\infty} C_{kp}^{(n)} \frac{f(\epsilon_p)}{f(\epsilon_k)} \phi_p .$$

APPENDIX B

This appendix outlines the derivation of Eq. (3.28). For notational simplicity, we combine the particle-hole and hole-hole components of the wave functions (3.21) at iteration n,

$$\phi_k^{(n)} = \phi_k + \sum_{a \neq k} C_{ka}^{(n)} \phi_a \quad (k = 1, 2, \ldots, A) .$$

Assume that the filter $f(\hat{h})$ admits a Taylor expansion

$$f(\hat{h}) = \sum_{v=0}^{\infty} f_v \hat{h}^{v} .$$

Then, keeping only first order terms in $\delta^{(n)}V$,

$$f(\hat{h}^{(n)}) = \sum_{v=0}^{\infty} f_v (\hat{h} + \delta V^{(n)})^v$$

$$= f(\hat{h}) + \sum_{v=0}^{\infty} \sum_{j=0}^{v-1} f_v \hat{h}^{v-1-j} \delta V^{(n)} \hat{h}^{j} .$$

Therefore

$$f(\hat{h}^{(n)})\phi_k^{(n)} = \sum_{v=0}^{\infty} f_v \left[\epsilon_k^v \phi_k + \sum_{a \neq k} C_{ka}^{(n)} \epsilon_a^v \phi_a \right]$$

$$+ \sum_{v=0}^{\infty} \sum_{j=0}^{v-1} f_v \hat{h}^{v-1-j} \delta V^{(n)} \hat{h}^{j} \phi_k ,$$

so that, with the notation in Eq. (3.27),

$$f(\hat{h}^{(n)})\phi_k^{(n)} = \sum_{a} \mathcal{C}_{ka} \phi_a ,$$

we obtain

$$\mathcal{C}_{kk} = \langle k | f(\hat{h}^{(n)}) | \phi_k^{(n)} \rangle = \sum_{v=0}^{\infty} f_v \epsilon_k^v + \sum_{v=0}^{\infty} \sum_{j=0}^{v-1} f_v \langle k | \hat{h}^{v-1-j} \delta V^{(n)} \hat{h}^{j} | k \rangle$$

$$= f(\epsilon_k) + \sum_{v=0}^{\infty} f_v v \langle k | \delta V^{(n)} | k \rangle \epsilon_k^{v-1} = f(\epsilon_k) + \langle k | \delta V^{(n)} | k \rangle f'(\epsilon_k) .$$

Similarly, for $\alpha \neq k$,

$$\mathscr{C}_{k\alpha} = \langle \alpha | f(\hat{h}^{(n)}) | \phi_k^{(n)} \rangle = \sum_{\nu=0}^{\infty} f_\nu C_{k\alpha}^{(n)} \epsilon_\alpha^\nu + \sum_{\nu=0}^{\infty} \sum_{j=0}^{\nu-1} f_\nu \langle \alpha | \hat{h}^{\nu-1-j} \delta V^{(n)} \hat{h}^j | k \rangle$$

$$= C_{k\alpha}^{(n)} f(\epsilon_\alpha) + \sum_{\nu=0}^{\infty} \sum_{j=0}^{\nu-1} f_\nu \epsilon_\alpha^{\nu-1-j} \epsilon_k^j \langle \alpha | \delta V^{(n)} | k \rangle$$

$$= C_{k\alpha}^{(n)} f(\epsilon_\alpha) + \langle \alpha | \delta V^{(n)} | k \rangle [f(\epsilon_\alpha) - f(\epsilon_k)] / (\epsilon_\alpha - \epsilon_k) ,$$

where the identity $(\epsilon_\alpha^\nu - \epsilon_k^\nu)/(\epsilon_\alpha - \epsilon_k) = \sum_{j=0}^{\nu-1} \epsilon_k^{\nu-1-j} \epsilon_k^j$ has been used.

APPENDIX C

Here, we illustrate the basic idea for the removal of a sawtooth instability. Let us consider a Hartree filter in which the potential is calculated from a linear combination of the densities at iterations n and $n-1$,

$$\rho(x) = \frac{\rho^{(n)}(x) + \zeta \rho^{(n-1)}(x)}{1+\zeta} , \tag{C1}$$

where ζ is a mixing parameter. Heuristically, it is plausible that a noise term which alternates in sign at each iteration will be damped by averaging the densities at two subsequent iterations. The effect of this mixing may be analyzed quantitatively by expanding the potential in the vicinity of a fixed point,

$$V^{(n)}(x) = V(x) + \int dy [\nu(x-y) + 2V_\delta \rho(x) \delta(x-y)]$$
$$\times \frac{\delta \rho^{(n)}(y) + \zeta \delta \rho^{(n-1)}(y)}{1+\zeta} , \tag{C2}$$

and applying perturbation theory as in (3.49) to obtain

$$C_{kp}^{(n+1)} = S_{kp,jq} \frac{C_{jq}^{(n)} + \zeta C_{jq}^{(n-1)}}{1+\zeta} + T_{kp,jq} \frac{C_{jq}^{(n)} + \zeta C_{jq}^{(n-1)}}{1+\zeta} . \tag{C3}$$

Now, consider a single sawtooth mode for which the normal stability matrix (with $\zeta=0$) has an eigenvalue $S = 1 - \lambda$ less than -1. The recursion relation for this mode with mixing parameter ζ is then

$$C^{(n+1)} = \frac{S}{1+\zeta} C^{(n)} + \frac{\zeta S}{1+\zeta} C^{(n-1)} , \tag{C4}$$

which may be written in the matrix form

$$\begin{bmatrix} C^{(n+1)} \\ C^{(n)} \end{bmatrix} = \begin{bmatrix} S(1+\zeta) & \zeta S/(1+\zeta) \\ 1 & 0 \end{bmatrix} \begin{bmatrix} C^{(n)} \\ C^{(n-1)} \end{bmatrix} . \tag{C5}$$

The eigenvalues of the matrix appearing in (C5) are

$$\lambda = \frac{S}{2(1+\zeta)} \left\{ 1 \pm \left[1 + \frac{4\zeta(1+\zeta)}{S} \right]^{1/2} \right\} ,$$

with the three significant limits

$$\lambda(\zeta \to 0) \sim \begin{cases} S + \zeta(1-S) \\ -\zeta , \end{cases}$$

$$\lambda \left[\zeta_1 = \frac{1+S}{S-1} \right] = \begin{cases} -1 \\ (1+S)/2 , \end{cases} \tag{C6}$$

$$\lambda \left[\zeta_2 = \frac{\sqrt{1-S}-1}{2} \right] = \frac{S}{2(1+\zeta)} .$$

Thus, the two roots start at the values S and 0 and approach each other as ζ increases. At the value $\zeta_1 = (1+S)/(S-1)$, the most negative root has increased to -1 and hence becomes stable. As long as $-3 < S$, the root which is decreasing from 0 has not yet crossed the lower root and thus both modes are stable. Eventually, as ζ is increased further, the two roots merge at ζ_2, after which the modulus is given by $|\lambda|^2 = -S\zeta/(1+\zeta)$ and the algorithm finally becomes unstable again for sufficiently large ζ. Thus, we conclude that instabilities associated with eigenvalues of the filter stability matrix in the range $-3 < S < -1$ may be removed by appropriate choice of the mixing parameter ζ. In practice, of course, one uses the smallest possible value, ζ_1, since the mixing also pushes the most positive eigenvalue closer to 1 and thus slows convergence. Admixtures of more iterations may be used to treat a larger range of negative eigenvalues.

*Present address: Istituto di Fisica Dell Università de Cagliari, via Ospedale 72, Cagliari, Italy

[1]J. W. Negele, Rev. Mod. Phys. **54**, 913 (1982).

[2]S. Levit, J. W. Negele, and Z. Paltiel, Phys. Rev. C **22**, 1979 (1980).

[3]H. Reinhardt, Nucl. Phys. **A367**, 269 (1981).

[4]J. W. Negele and H. Orland, *Quantum Many Particle Systems* (Benjamin/Cummings, Reading, MA, in press).

[5]J. P. Blaizot and H. Orland, Phys. Rev. C **24**, 1740 (1981).

[6]B. Bonche, S. E. Koonin, and J. W. Negele, Phys. Rev. C **13**, 1226 (1976).

[7]D. J. Thouless, *The Quantum Mechanics of Many-Body Systems* (Academic, New York, 1972).

[8]S. Levit, private communication.

[9]M. A. Preston and R. K. Bhaduri, *Structure of the Nucleus* (Addison-Wesley, Reading, MA 1975), Chap. 5.